Modern advances in galactic astrophysics : from *scale-invariant dynamics* to a successful theory of galaxy formation and evolution

Lecture 4

Correlations in the properties of galaxies II.
Evidence for a new law of nature : space-time scale invariant dynamics. Some steps towards a deeper theoretical understanding.

12.01.2017

Selected Chapters on Astrophysics
Charles University, Praha,
December & January 2016/17

Pavel Kroupa
Helmholtz-Institute for Radiation und Nuclear Physics (HISKP)
University of Bonn

Astronomical Institute,
Charles University in Prague

c/o Argelander-Institut für Astronomie
University of Bonn

Lecture 1 (14.12.16) **:**

The standard model of cosmology (SMoC) and the arguably greatest question of 20th/21st century physics : Do the postulated dark matter particles exist ?

Lecture 2 (21.12.16) **:**

Further on dynamical friction : evidence for merging galaxies.
Galaxy populations.

Lecture 3 (04.01.17) **:**

Structures on large scales and performance of the SMoC;
Correlations in the properties of galaxies I : Galaxies are simple systems.

Lecture 4 (11.01.17) **:**

Correlations in the properties of galaxies II.
Evidence for a new law of nature : space-time scale-invariant dynamics.
Some steps towards a deeper theoretical understanding.

Remember:

Distribution of matter on 100kpc, 3Mpc, 8 Mpc and 800Mpc scales
=> *incompatibility with SMoC.*

Evidence for anisotropies (SNIa-based cosmological solutions, galaxy morphology distribution, GRB distribution, CMB anomalies)
=> *incompatibility with SMoC.*

Theory confidence graph based on >29 failures
=> reject *SMoC with >99.9968 per cent confidence .*

How to proceed?**:** **1.** It seems reasonable to assume the SMoC is falsified.
2. Study the vastly dominant galaxy population (disk galaxies) to hopefully infer the effective laws of nature relevant for cosmology.

Disk galaxies **:** **a)** Exponential disks.
b) Strong correlations between stellar mass and radius, gas mass.

Continue with properties of disk galaxies :

The main sequence of galaxies :

a strong correlation between stellar mass and the SFR of the galaxy.

Remember: >90% of all galaxies locally and 6 Gyr ago with stellar mass $> 10^{10}\, M_\odot$ are star-forming disk galaxies. These lie on a "main sequence":

$$\log_{10}(SFR) = \alpha \log_{10}(M_*) + \beta$$

α, β are constants, which depend on the redshift z

Speagle, Steinhardt, Capak, Silverman 2014

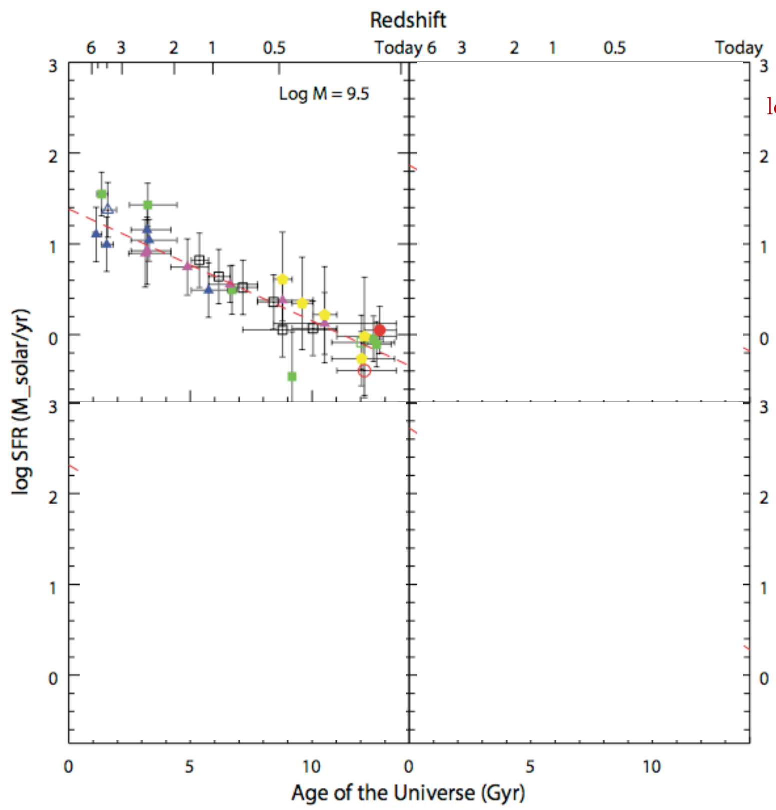

$\log_{10}(SFR) = \alpha \log_{10}(M_*) + \beta$

Speagle, Steinhardt, Capak, Silverman 2014

FIG. 4.— $\log \psi$ vs. t for $\log M_* = (9.5, 10.0, 10.5, 11.0)$, calculated using the best fit MS relations from each of the 25 studies listed in Table 3 and plotted using the same color/symbol scheme as Figure 2. The best fits (excluding non-selective data; see Figure 1 and §4) for a given mass are plotted as red dashed lines.

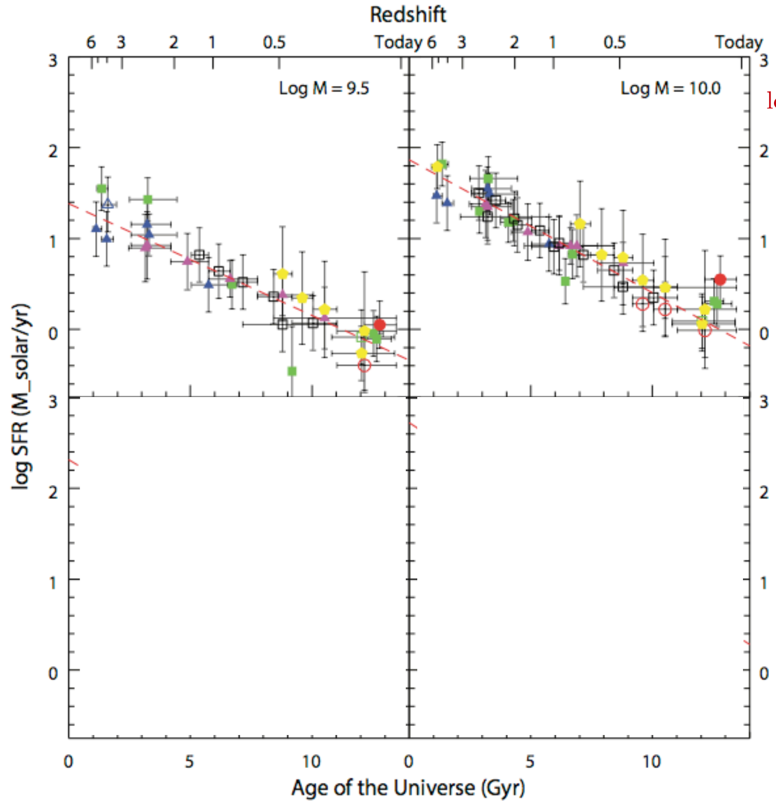

$\log_{10}(SFR) = \alpha \log_{10}(M_*) + \beta$

Speagle, Steinhardt, Capak, Silverman 2014

FIG. 4.— log ψ vs. t for log M_* = (9.5, 10.0, 10.5, 11.0), calculated using the best fit MS relations from each of the 25 studies listed in Table 3 and plotted using the same color/symbol scheme as Figure 2. The best fits (excluding non-selective data; see Figure 1 and §4) for a given mass are plotted as red dashed lines.

Evolution of the Star-forming Main Sequence 17

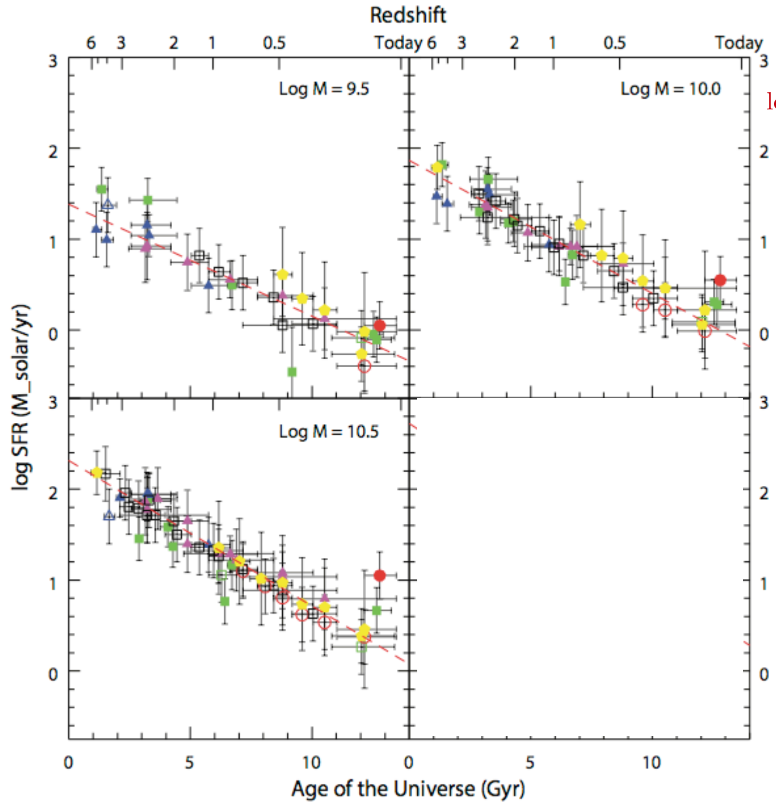

$\log_{10}(SFR) = \alpha \log_{10}(M_*) + \beta$

Speagle, Steinhardt, Capak, Silverman 2014

FIG. 4.— log ψ vs. t for log M_* = (9.5, 10.0, 10.5, 11.0), calculated using the best fit MS relations from each of the 25 studies listed in Table 3 and plotted using the same color/symbol scheme as Figure 2. The best fits (excluding non-selective data; see Figure 1 and §4) for a given mass are plotted as red dashed lines.

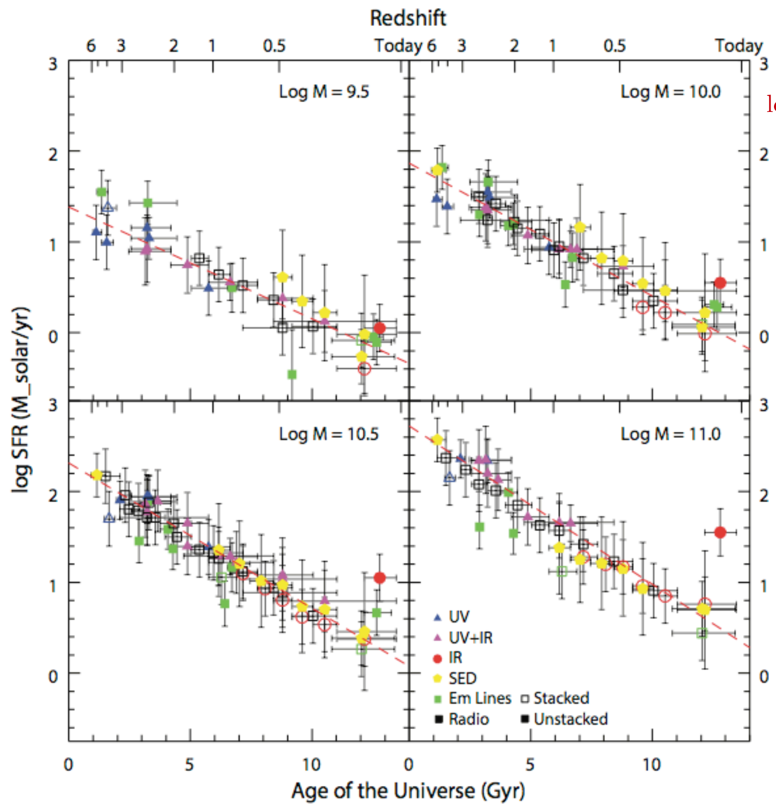

$$\log_{10}(SFR) = \alpha \log_{10}(M_*) + \beta$$

Speagle, Steinhardt, Capak, Silverman 2014

FIG. 4.— $\log \psi$ vs. t for $\log M_* = (9.5, 10.0, 10.5, 11.0)$, calculated using the best fit MS relations from each of the 25 studies listed in Table 3 and plotted using the same color/symbol scheme as Figure 2. The best fits (excluding non-selective data; see Figure 1 and §4) for a given mass are plotted as red dashed lines.

$$\log_{10}(SFR) = \alpha(t) \log_{10}(M_*) + \beta(t)$$

$$\log_{10}(SFR) = [0.84 \pm 0.02 - 0.026 \pm 0.003 \times t] \log_{10}(M_*) - [6.51 \pm 0.24 - 0.11 \pm 0.03 \times t]$$

(note the small scatter !)

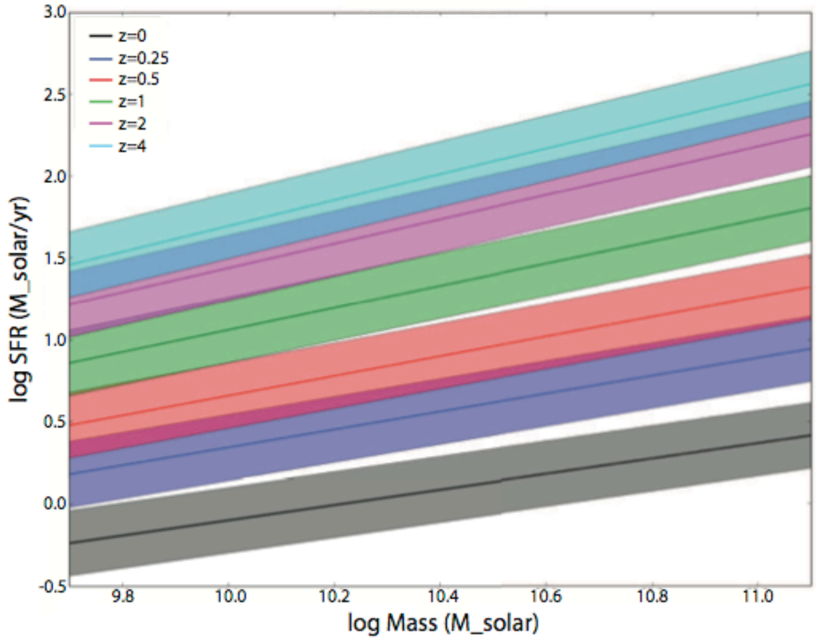

Speagle, Steinhardt, Capak, Silverman 2014

FIG. 8.— Several of our "consensus" MS relations taken from our best fit to observations from the literature (see §5.1) plotted at several given redshifts. The widths of the distributions are taken to be the "true" scatters (±0.2 dex) rather than the likely observed scatters (~ 0.3 dex) for improved clarity, and the mass bounds are taken directly from the fit. The changing MS slope and ~ 2 orders of magnitude evolution in SFR at fixed mass from $z = 4$ to 0 are easily visible. As the first and last 2 Gyrs of data are not included in the fit, the $z = 0$ and $z = 4$ slopes should be viewed as predictions of high-/low-z MS relations rather than simply best fits to data available at those redshifts (which would tend to fit well by default).

$$\log_{10}(SFR) = \alpha(t)\log_{10}(M_*) + \beta(t)$$

$$\log_{10}(SFR) = [0.84 \pm 0.02 - 0.026 \pm 0.003 \times t]\log_{10}(M_*) - [6.51 \pm 0.24 - 0.11 \pm 0.03 \times t]$$

(note the small scatter !)

How does this fit with the stochastic haphazard merger-driven buildup of galaxies following the merger tree in the standard (dark matter) model **?**

Problems **:**

a) Write down an equation for the main sequence of galaxies in terms of the galaxy- wide star formation rate, SFR, and the mass in stars of the galaxy, M_*, and with the two parameters α and β.

b) Assuming the two parameters α,β to be constants of time and mass and taking $SFR = dM_*/dt$, how does the stellar mass of a galaxy evolve over time if a galaxy is on the main sequence **?** Assume no limitations on the accreted gas reservoir.

Disk galaxies thus obey strong correlations between their stellar masses, gas masses, their radii**,**
and (surprisingly), their SFRs !

Disk galaxies also obey a very strong correlation between their baryonic (stellar + gas) mass and the rotation speed of the flat (and extended) part of their rotation curve **. . .**

The observational Baryonic Tully -Fisher Relation (BTFR)

Famaey & McGaugh 2012

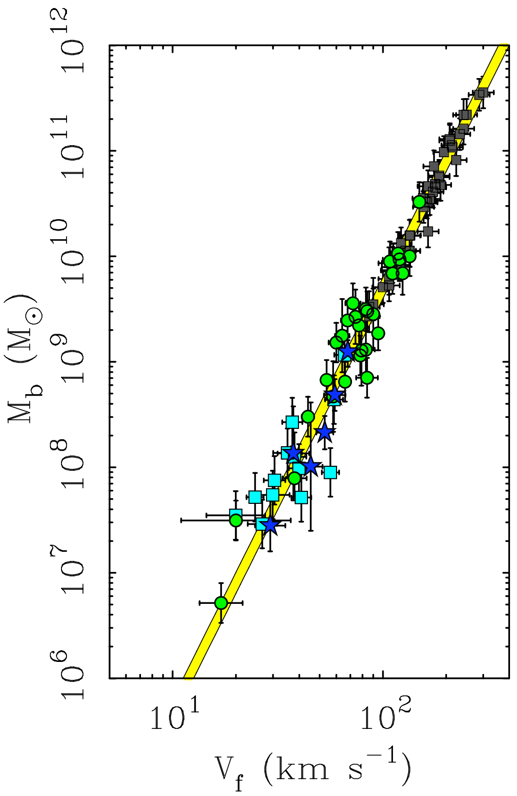

The observational Baryonic Tully -Fisher Relation (BTFR)

Bayesian inference from the K-band luminosity function 37

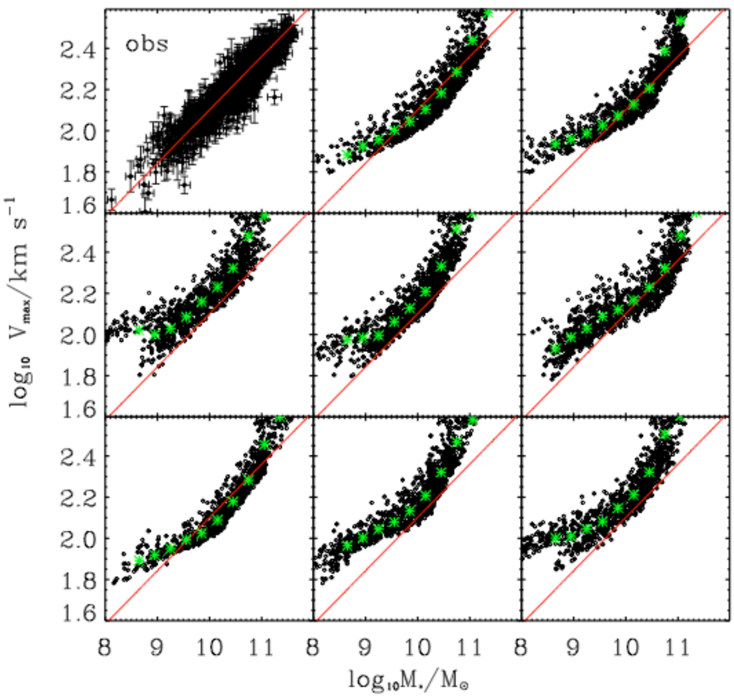

Figure 4. The stellar mass Tully-Fisher relation predicted by 8 models randomly selected from the posterior compared with data from Dutton et al. (2011) shown in the upper-left panel. The red line denotes a fit to the observational data given by Dutton et al. (2011).

Lu, Mo, Katz & Weinberg 2012

Curvature in SMoC models because accretion of gas onto galaxy is governed by the DM halo **:**

massive DM halo ==> fast/hot accretion

low-mass DM halo ==> slow/cold accretion ==> "inefficient" galaxy formation

Observed BTF linear ==> no DM halos **?**

The observational Baryonic Tully -Fisher Relation (BTFR)

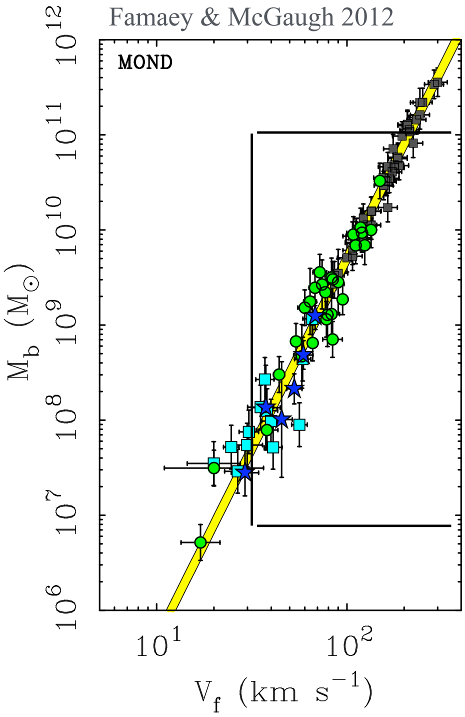

The observational Baryonic Tully -Fisher Relation (BTFR)

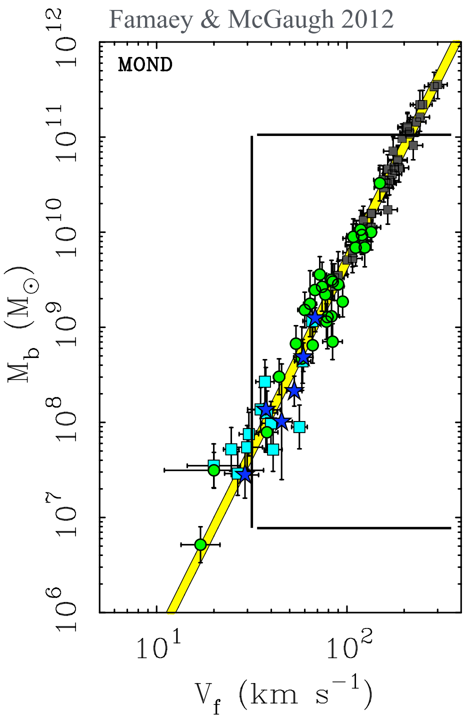

EAGLI
project
Sales, Nav
et al. 201
MNRA

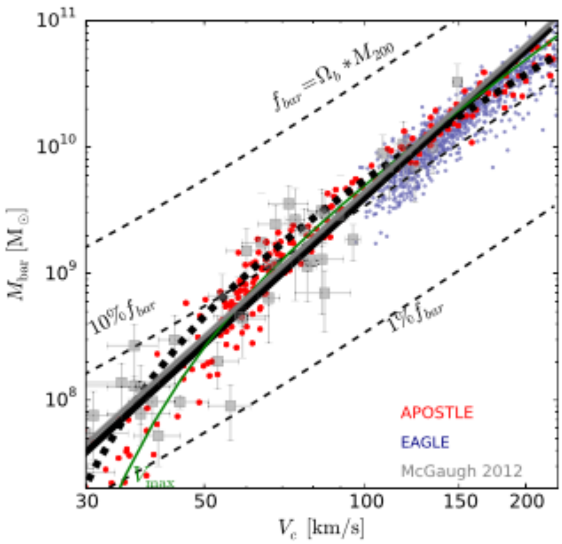

Figure 4. Simulated BTF relation for galaxies with circular velocities in the range $30 < V_c$ / km s^{-1}/<230. Symbols and colours are as in Fig. 3. We use the circular velocity at $2\,r_h^{bar}$ for simulated galaxies. Grey symbols with error bars show data from the observational compilation of McGaugh (2012) that use the asymptotic 'flat' rotation velocity. Simulations and observations are generally in good agreement. Solid lines indicate the best power-law fits to simulations (black) and observations (grey). The thick black dashed line is a fit to simulated data with steepening slope at the faint end. Parameters of the fit are listed in Table 2. The green thin curve depicts the relation between baryonic mass and the maximum circular velocity of the haloes in our simulations. Note that the slope of the simulated BTF relation is steeper than V^3, as a result of the declining galaxy formation efficiency in low-mass haloes shown in Fig. 1.

MNRAS **464**, 2419–2428 (2017)
Advance Access publication 2016 September 28
doi:10.1093/mnras/stw2461

The low-mass end of the baryonic Tully–Fisher relation

Laura V. Sales,[1★] Julio F. Navarro,[2†] Kyle Oman,[2] Azadeh Fattahi,[2] Ismael Ferrero,[3,4] Mario Abadi,[3,4] Richard Bower,[5] Robert A. Crain,[6] Carlos S. Frenk,[5] Till Sawala,[7] Matthieu Schaller,[5] Joop Schaye,[8] Tom Theuns[5] and Simon D. M White[9]

ABSTRACT

The scaling of disc galaxy rotation velocity with baryonic mass (the 'baryonic Tully–Fisher' relation, BTF) has long confounded galaxy formation models. It is steeper than the $M \propto V^3$ scaling relating halo virial masses and circular velocities and its zero-point implies that galaxies comprise a very small fraction of available baryons. Such low galaxy formation efficiencies may, in principle, be explained by winds driven by evolving stars, but the tightness of the BTF relation argues against the substantial scatter expected from such a vigorous feedback mechanism. We use the APOSTLE/EAGLE simulations to show that the BTF relation is well reproduced in Λcold dark matter (CDM) simulations that match the size and number of galaxies as a function of stellar mass. In such models, galaxy rotation velocities are proportional to halo virial velocity and the steep velocity-mass dependence results from the decline in galaxy formation efficiency with decreasing halo mass needed to reconcile the CDM halo mass function with the galaxy luminosity function. The scatter in the simulated BTF is smaller than observed, even when considering all simulated galaxies and not just rotationally supported ones. The simulations predict that the BTF should become increasingly steep at the faint end, although the velocity scatter at fixed mass should remain small. Observed galaxies with rotation speeds below $\sim$40 km s^{-1} seem to deviate from this prediction. We discuss observational biases and modelling uncertainties that may help to explain this disagreement in the context of ΛCDM models of dwarf galaxy formation.

?

It is unfortunately the case that these teams appear re-invent reality too "fit" their models.

The observational Baryonic Tully -Fisher Relation (BTFR)

Famaey & McGaugh 2012

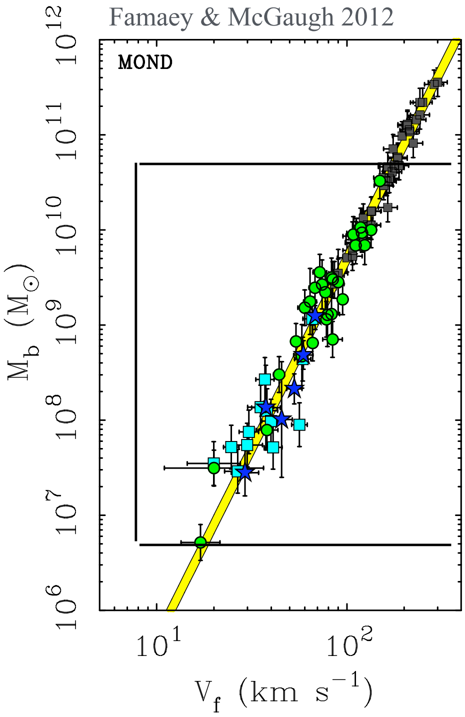

EAGLE project: Sales, Navarro et al. 2016, MNRAS

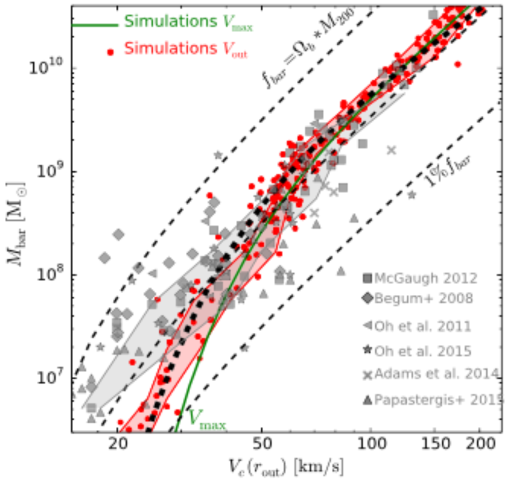

Figure 7. Comparison between predicted and observed baryonic Tully–Fisher relations, extended to include fainter galaxies than in Fig. 4. Grey symbols indicate the observed compilation, from references listed in the legend. Velocities are now defined at r_{out}, the outermost point of the observed rotation curve given in Fig. 6 (or its maximum value, when the two do not coincide). Median values of maximum velocity at given baryonic mass for simulated galaxies are indicated by the thick solid line labelled 'V_{max}'. Small dots indicate the predicted velocities of simulated galaxies measured at the r_{out} based on the best power-law fit to the observed sample (see green line in Fig. 6). The shaded areas correspond to the interquartile velocity range at a given fixed baryonic mass for the simulated (red) and observed (grey) samples. As expected from Fig. 6, $V_c(r_{out})$ underestimates the maximum velocity in low-mass galaxies by a factor of ≈1.5. Note as well that the simulated BTF shows a clear steepening in mass at the faint end that is less pronounced in the observed BTF. The observed BTF also has substantially larger scatter at the faint end, with a number of clear outliers with no counterparts in the simulated sample (see the text for more details).

The *theoretical BTFR* thus has too much scatter at high-mass end (at low mass end the observational data have significantly larger observational uncertainty and thus an apparently larger scatter) and the *theoretical BTFR* has curvature.

The observed rotation curves also do not match the theoretical ones.
(Wu & Kroupa 2015)

The rare elliptical galaxies also follow similar correlations between stellar mass, radius, mass-to-light ratio, age of stellar population, velocity dispersion (the Faber-Jackson Relation)

(e.g. Dabringhausen et al. 2008).

The rare elliptical galaxies also follow similar correlations between stellar mass, radius, mass-to-light ratio, age of stellar population, velocity dispersion (the Faber-Jackson Relation)

(e.g. Dabringhausen et al. 2008).

A&A 581, A98 (2015)
DOI: 10.1051/0004-6361/201526879

Astronomy & Astrophysics

The H I Tully-Fisher relation of early-type galaxies

Milan den Heijer[1,2,⋆], Tom A. Oosterloo[3,4], Paolo Serra[5], Gyula I. G. Józsa[6,7,1], Jürgen Kerp[1], Raffaella Morganti[3,4], Michele Cappellari[8], Timothy A. Davis[9], Pierre-Alain Duc[10], Eric Emsellem[11], Davor Krajnović[12], Richard M. McDermid[13,14], Torsten Naab[15], Anne-Marie Weijmans[16], and P. Tim de Zeeuw[11,17]

ABSTRACT

We study the H I K-band Tully-Fisher relation and the baryonic Tully-Fisher relation for a sample of 16 early-type galaxies, taken from the ATLAS^{3D} sample, which all have very regular H I disks extending well beyond the optical body ($\gtrsim 5\,R_{\rm eff}$). We use the kinematics of these disks to estimate the circular velocity at large radii for these galaxies. We find that the Tully-Fisher relation for our early-type galaxies is offset by about 0.5−0.7 mag from the relation for spiral galaxies, in the sense that early-type galaxies are dimmer for a given circular velocity. The residuals with respect to the spiral Tully-Fisher relation correlate with estimates of the stellar mass-to-light ratio, suggesting that the offset between the relations is mainly driven by differences in stellar populations. We also observe a small offset between our Tully-Fisher relation with the relation derived for the ATLAS^{3D} sample based on CO data representing the galaxies' inner regions ($\lesssim 1\,R_{\rm eff}$). This indicates that the circular velocities at large radii are systematically 10% lower than those near 0.5−1 $R_{\rm eff}$, in line with recent determinations of the shape of the mass profile of early-type galaxies. The baryonic Tully-Fisher relation of our sample is distinctly tighter than the standard one, in particular when using mass-to-light ratios based on dynamical models of the stellar kinematics. We find that the early-type galaxies fall on the spiral baryonic Tully-Fisher relation if one assumes $M/L_K = 0.54\,M_\odot/L_\odot$ for the stellar populations of the spirals, a value similar to that found by recent studies of the dynamics of spiral galaxies. Such a mass-to-light ratio for spiral galaxies would imply that their disks are 60−70% of maximal. Our analysis increases the range of galaxy morphologies for which the baryonic Tully-Fisher relations holds, strengthening previous claims that it is a more fundamental scaling relation than the classical Tully-Fisher relation.

The rare elliptical galaxies also follow similar correlations between stellar mass, radius, mass-to-light ratio, age of stellar population, velocity dispersion (the Faber-Jackson Relation)
(e.g. Dabringhausen et al. 2008).

den Heijer, Oosterloo et al. 2015, A&A

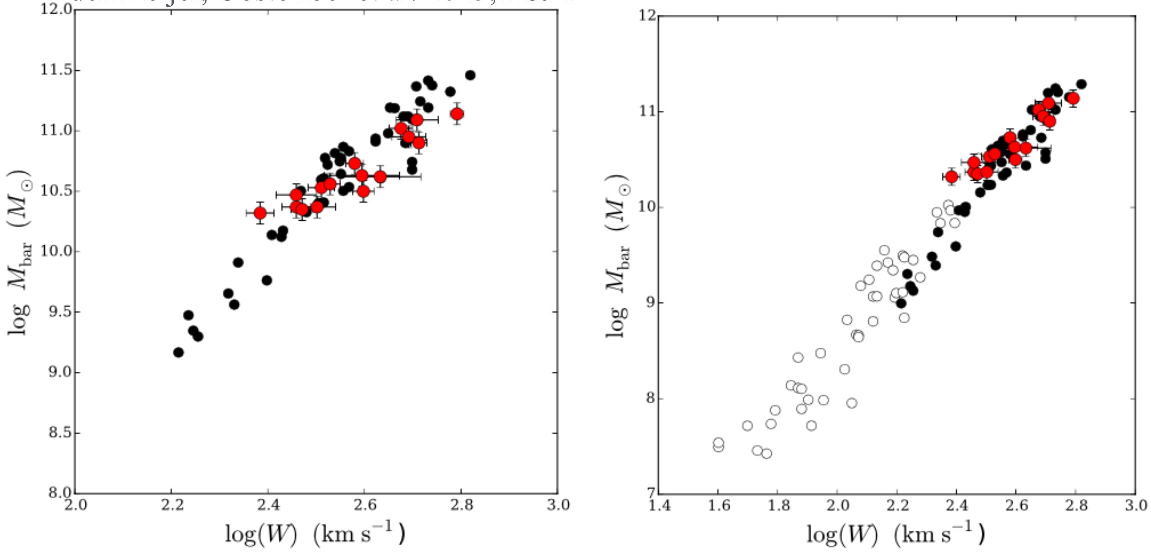

Fig. 11. Baryonic TFR where the galaxy masses for our sample galaxies are estimated using $M/L_{\rm JAM}$. The red symbols represent our ATLAS$^{\rm 3D}$ sample, the black symbols are the data from Noordermeer & Verheijen (2007), while the open symbols show the data from McGaugh (2012) for gas-dominated galaxies. For the data from Noordermeer & Verheijen (2007) in the *left-hand panel* $M/L_K = 0.8\ M_\odot/L_\odot$ was used, as in the original Noordermeer & Verheijen (2007) paper, while in the *right-hand panel* $M/L_K = 0.54\ M_\odot/L_\odot$ was used. The scaling of the lefthand figure is the same as that of Fig. 7 to facilitate easy comparison.

The rare elliptical galaxies also follow similar correlations between stellar mass, radius, mass-to-light ratio, age of stellar population, velocity dispersion (the Faber-Jackson Relation)
(e.g. Dabringhausen et al. 2008; 2016).

Galaxies thus obey a very strong correlation between the internal radial acceleration and the "mass-discrepancy" . . .

The clue to an extension of the law of gravity ?

Mass-Discrepancy correlation with acceleration

The Sanders-McGaugh correlation

Sanders 1990; McGaugh 2004
Famaey & McGaugh 2012
(Kroupa 2012, 2015)

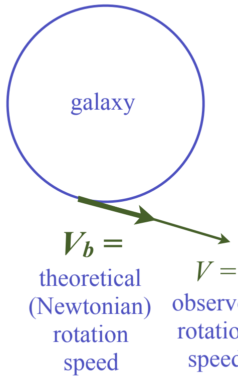

Mass-Discrepancy correlation with acceleration

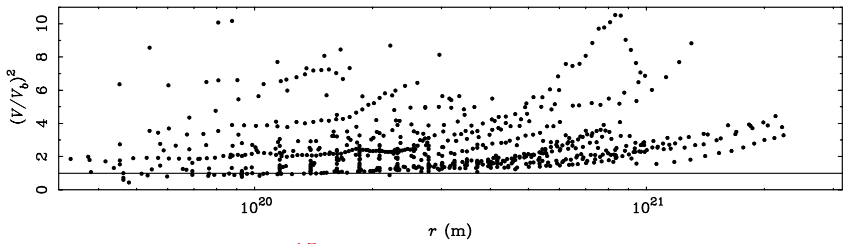

$1\ \mathrm{pc} = 31 \times 10^{15}\ \mathrm{m}$ $\qquad$ $1\ \mathrm{m} = 3.2 \times 10^{-17}\ \mathrm{pc}$

Sanders 1990; McGaugh 2004
Famaey & McGaugh 2012
(Kroupa 2012, 2015)

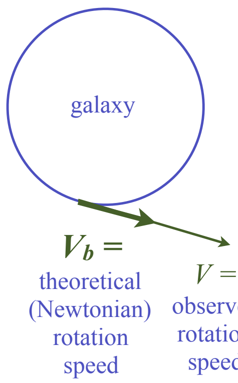

Mass-Discrepancy correlation with acceleration

Sanders 1990; McGaugh 2004
Famaey & McGaugh 2012
(Kroupa 2012, 2015)

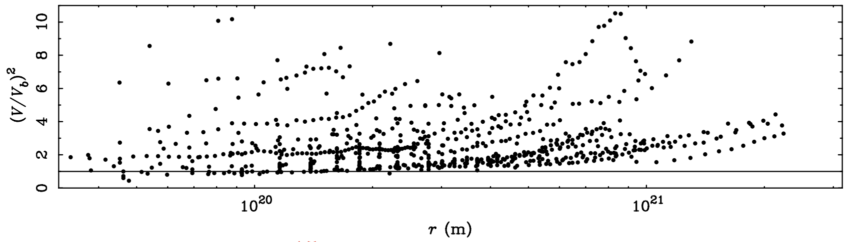

$1\ \text{pc} = 31 \times 10^{15}\ \text{m}$ $\quad$ $1\ \text{m} = 3.2 \times 10^{-17}\ \text{pc}$

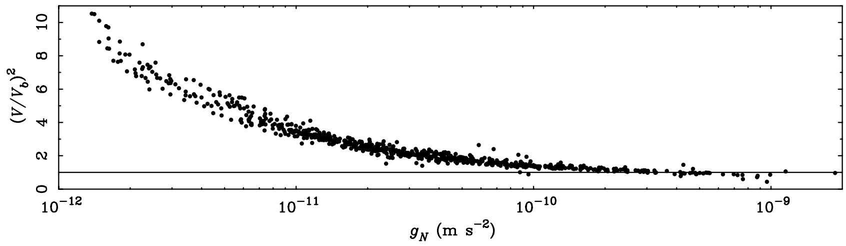

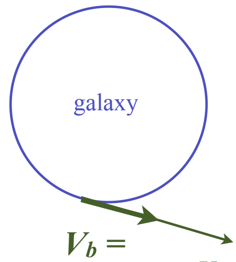

V_b = theoretical (Newtonian) rotation speed

V = observed rotation speed

Mass-Discrepancy correlation with acceleration

Sanders 1990; McGaugh 2004
Famaey & McGaugh 2012
(Kroupa 2012, 2015)

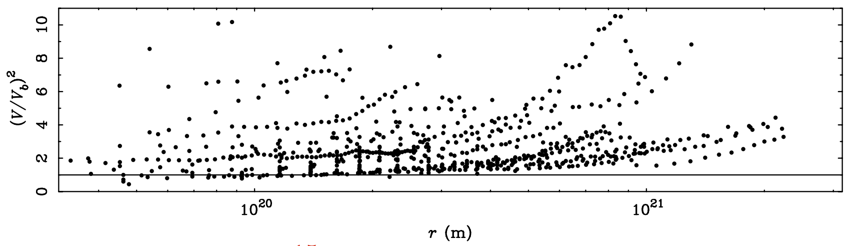

$1\ \text{pc} = 31 \times 10^{15}\ \text{m}$ $\quad$ $1\ \text{m} = 3.2 \times 10^{-17}\ \text{pc}$

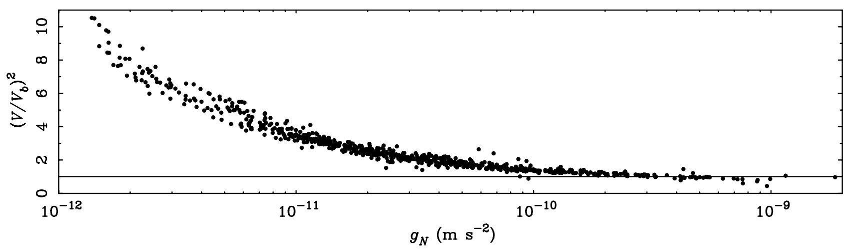

Correlation can't be explained by Dark Matter : DM particle physics is independent of the local acceleration in the SMoC.

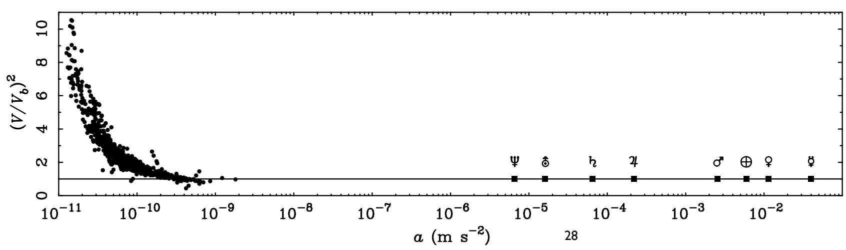

Mass-Discrepancy correlation with acceleration

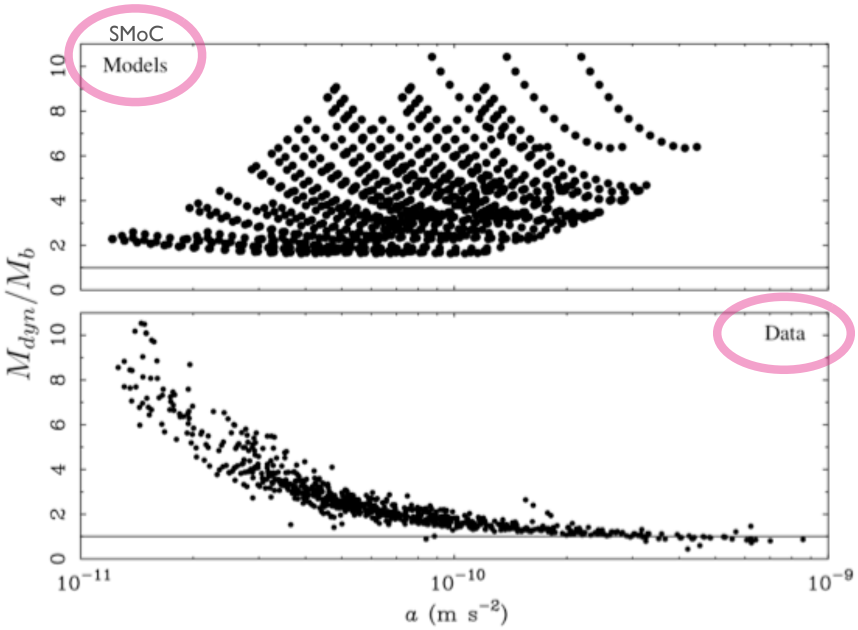

Fig. 3. The mass discrepancy–acceleration relation. The ratio of dynamical to baryonic mass is shown at each point along rotation curves as a function of the centripetal acceleration at that point. The top panel shows model galaxies in ΛCDM (see text). The bottom panel shows data for real galaxies (42). Individual galaxies, of which there are 74 here, do not distinguish themselves in this diagram, though model galaxies clearly do. The organization of the data suggest the action of a single effective force law in disk galaxies. This phenomenon does not emerge naturally from ΛCDM models.

$1\ \mathrm{pc} = 31 \times 10^{15}\ \mathrm{m}$ $\quad 1\ \mathrm{m} = 3.2 \times 10^{-17}\ \mathrm{pc}$

McGaugh 2014
also
Wu & Kroupa 2015

Correlation can't be explained by Dark Matter : DM particle physics is independent of the local acceleration in the SMoC.

Rotation curves / mass-discrepancy -- acceleration correlation

Wu & Kroupa 2015

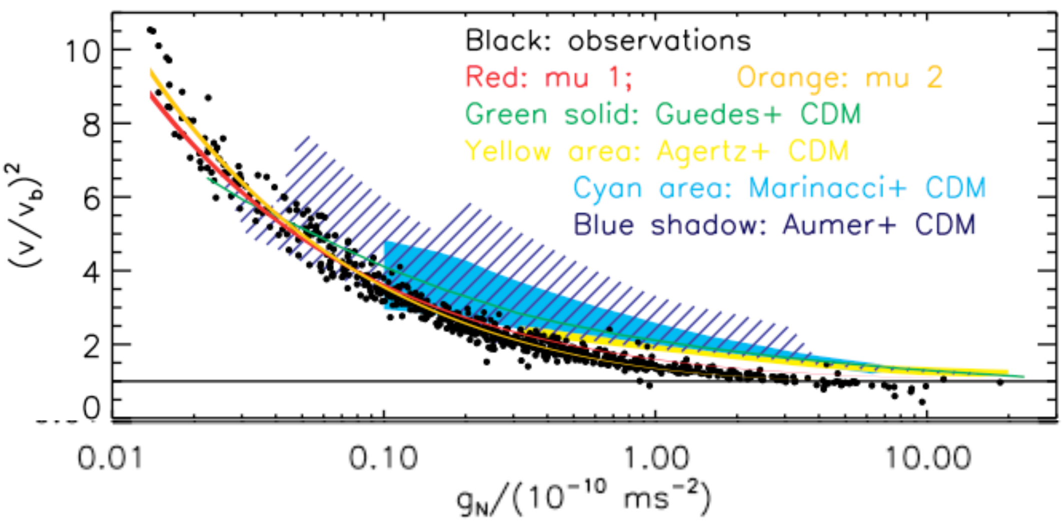

Neither cold nor warm dark matter models reproduce the observed data.

Thus, disk galaxies appear to be very simple systems : know stellar mass know essentially everything else (mass of HI, rotation velocity, radius, SFR).

This is a most remarkable and completely unexpected behaviour, _if_ galaxies are thought to form according to the cosmological merger tree.

"Galaxies appear simpler than expected"
Disney et al. (2008, Nature)

In the SMoC galaxies depend on :
- mass,
- spin of baryons,
- spin of dark matter halo,
- halo-concentration index,
- merger history,
- epoch of formation.

"... a process of hierarchical merging, in which the present properties of any galaxy are determined by the necessarily haphazard details of its last major mergers, hardly seems consistent with the very high degree of organization revealed in this analysis. "

"If, as we have argued, galaxies come from at most a six-parameter set, then for gaseous galaxies to appear as a one-parameter set, as observed here, the theory of galaxy formation and evolution must supply five independent constraint equations to constrain the observations. This is such a stringent set of requirements that it is hard to imagine any theory, *apart from the correct one*, fulfilling them all."

Which theory is this ?

It can hardly be the SMoC . . .

. . . thus,

the observational data disfavour the existence of dark matter

(SMoC leads to wrong structures
and lack of dynamical friction
disfavors dark matter particles)

The appearance of galaxies
is largely defined by
the law of gravitation . . .

A historical perspective which may give a clue . . .

Remember that Einstein constructed his GR to accommodate

Newton's *empirical* law of universal gravitation

1916. № 7.

ANNALEN DER PHYSIK.

VIERTE FOLGE. BAND 49.

1. ***Die Grundlage der allgemeinen Relativitätstheorie;***
von A. Einstein.

Die im nachfolgenden dargelegte Theorie bildet die denkbar weitgehendste Verallgemeinerung der heute allgemein als „Relativitätstheorie“ bezeichneten Theorie; die letztere nenne ich im folgenden zur Unterscheidung von der ersteren „spezielle Relativitätstheorie“ und setze sie als bekannt voraus. Die Verallgemeinerung der Relativitätstheorie wurde sehr erleichtert durch die Gestalt, welche der speziellen Relativitäts-

Einstein 1916

816 *A. Einstein.*

E. § 21. Newtons Theorie als erste Näherung.

Wie schon mehrfach erwähnt, ist die spezielle Relativitätstheorie als Spezialfall der allgemeinen dadurch charakterisiert, daß die $g_{\mu\nu}$ die konstanten Werte (4) haben. Dies bedeutet

Lichtes) bewegt ist, so kann man auf der rechten Seite Ableitungen nach der Zeit neben solchen nach den örtlichen Koordinaten vernachlässigen, so daß man erhält

$$\frac{d^2 x_\tau}{d t^2} = -\frac{1}{2}\frac{\partial g_{44}}{\partial x_\tau} \quad (\tau = 1, 2, 3). \qquad (67)$$

Dies ist die Bewegungsgleichung des materiellen Punktes nach Newtons Theorie, wobei $g_{44}/2$ die Rolle des Gravitationspotentiales spielt. Das Merkwürdige an diesem Resultat ist,

Remember that Einstein constructed his GR to accommodate

Newton's *empirical* law of universal gravitation

Remember that Einstein constructed his GR to accommodate

Newton's *empirical* law of universal gravitation

based on observational data limited entirely to the Solar System on a scale of Mercury to Neptune.

Remember that Einstein constructed his GR to accommodate

Newton's *empirical* law of universal gravitation

based on observational data limited entirely to the Solar System on a scale of Mercury to Neptune.

i.e.

over a spatial scale

$$s < 30\,\mathrm{AU} = 10^{-3.8}\,\mathrm{pc}$$

and an acceleration (space-curvature) scale

$$6 \times 10^{-6}\,\mathrm{m/s}^2 < g_\mathrm{N} < 4 \times 10^{-2}\,\mathrm{m/s}^2$$

> 6 orders of magnitude

Galaxies had not yet been discovered and they correspond to scales

$$s > 10^3\,\mathrm{pc}$$

$$g_\mathrm{N} < 10^{-9}\,\mathrm{m/s}^2$$

> 4 orders of magnitude

Should one expect an empirical law to hold over an extrapolation of orders of magnitude ?

Gedankenexperiment

by Indranil Banik (St. Andrews)

Depth of a trampolin with increasing weight :

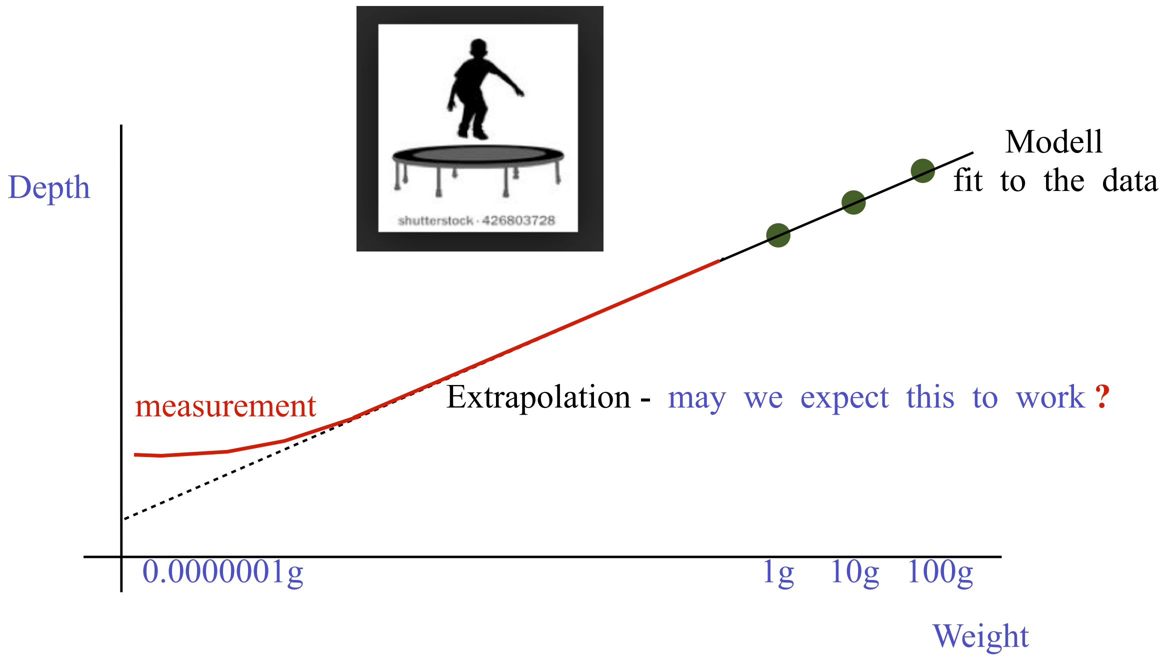

How to proceed ?

A clue is provided

by the

mass-discrepancy--acceleration data

in galaxies

Disc galaxies

Balance between gravitation and centrifugal force

Disc galaxies

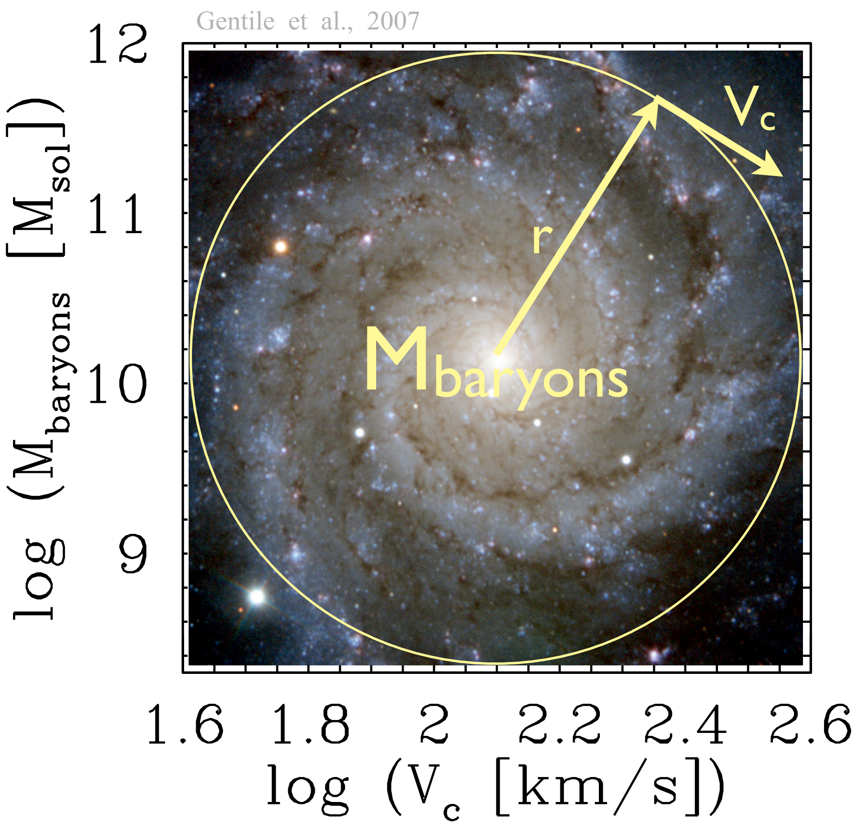

Balance between gravitation and centrifugal force

Nach Newton:

$$g_{\rm N} = G\,\frac{M_{\rm baryons}}{r^2}$$

Gemessen:

$$g = \frac{V_{\rm c}^2}{r}$$

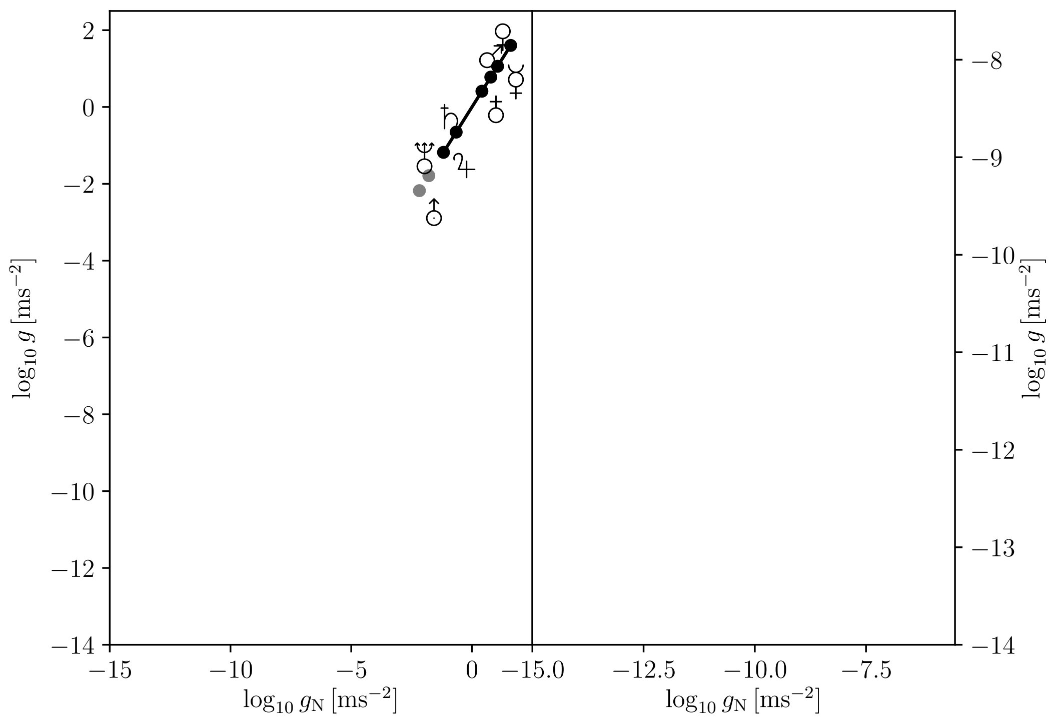

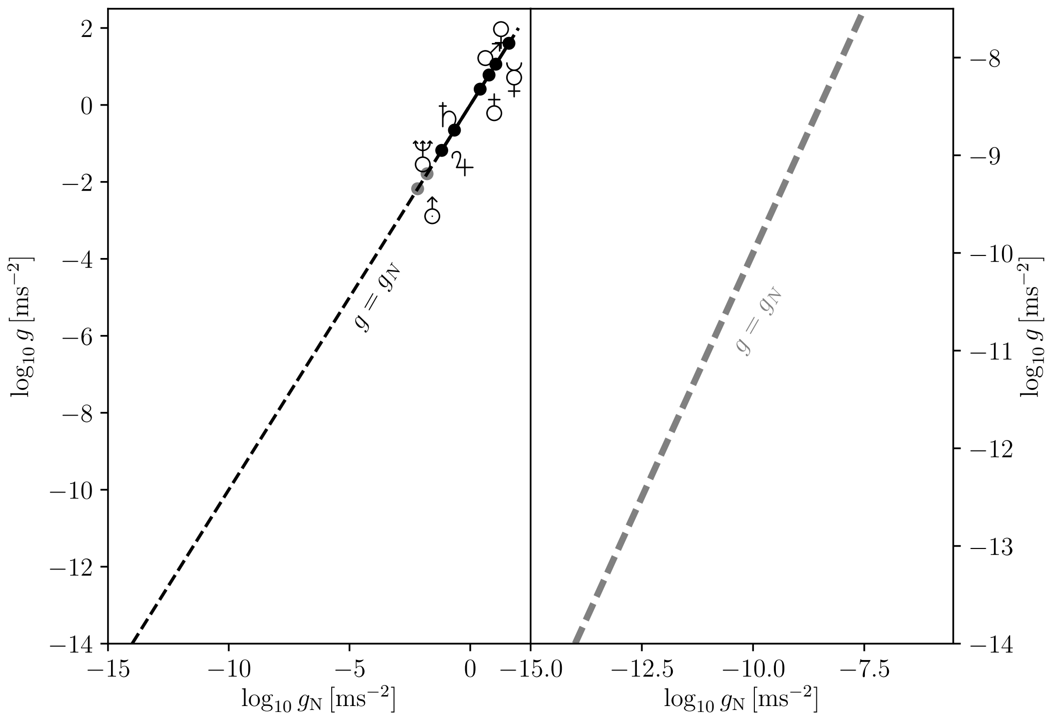

$\log_{10} g\,[\mathrm{ms}^{-2}]$
$\log_{10} g_N\,[\mathrm{ms}^{-2}]$
$g = g_N$

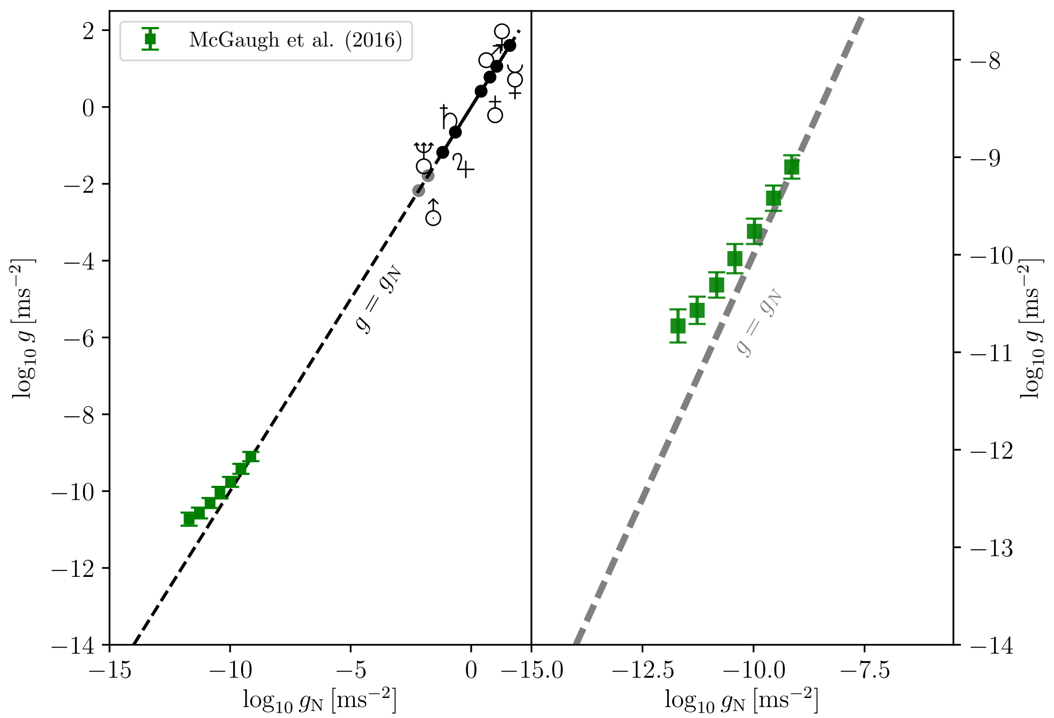

McGaugh et al. (2016)
$\log_{10} g\,[\mathrm{ms}^{-2}]$
$\log_{10} g_N\,[\mathrm{ms}^{-2}]$
$g = g_N$

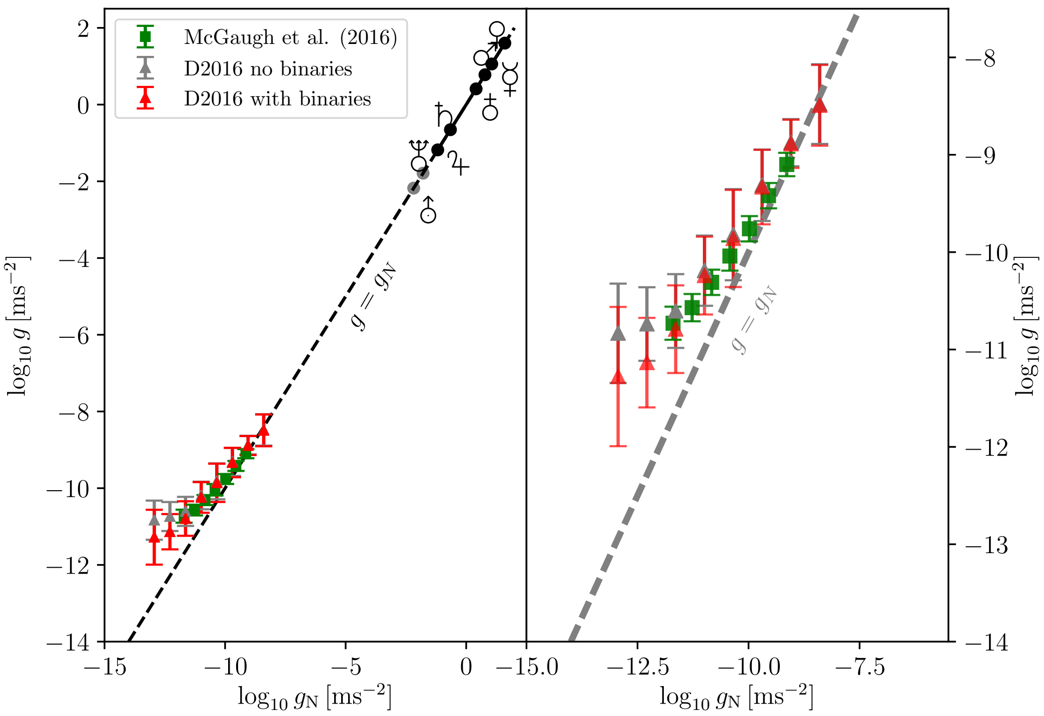

McGaugh et al. (2016)
D2016 no binaries
D2016 with binaries
$g = g_N$
$g = g_N$
$\log_{10} g\ [\mathrm{ms}^{-2}]$
$\log_{10} g_N\ [\mathrm{ms}^{-2}]$
$\log_{10} g_N\ [\mathrm{ms}^{-2}]$
$\log_{10} g\ [\mathrm{ms}^{-2}]$

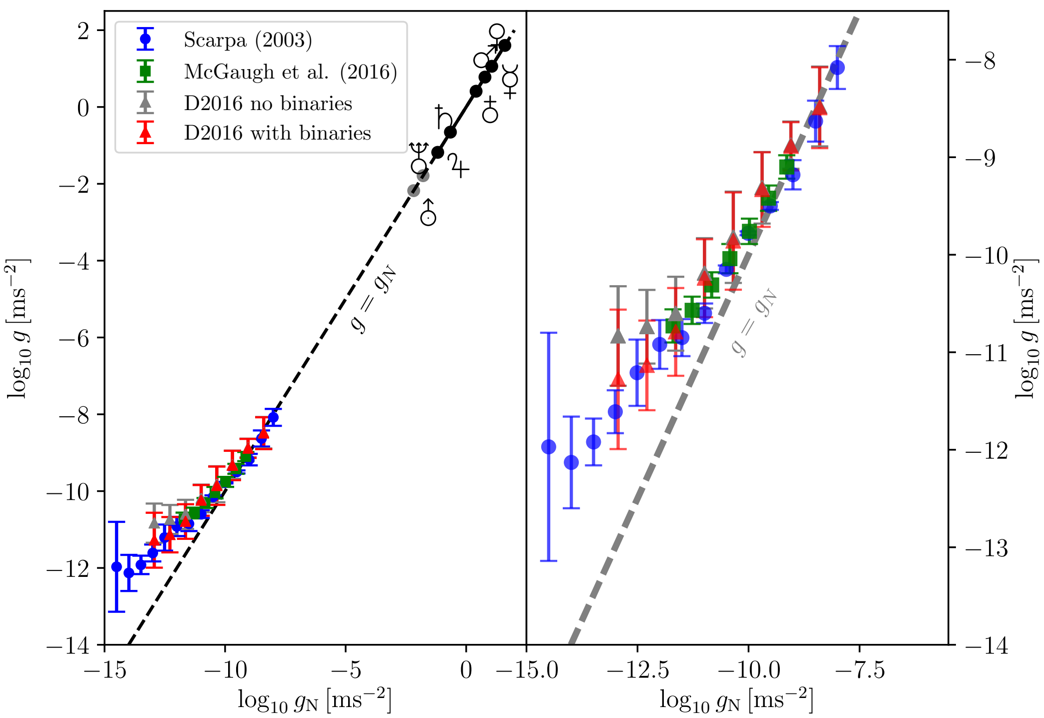

Scarpa (2003)
McGaugh et al. (2016)
D2016 no binaries
D2016 with binaries
$g = g_N$
$g = g_N$
$\log_{10} g\ [\mathrm{ms}^{-2}]$
$\log_{10} g_N\ [\mathrm{ms}^{-2}]$
$\log_{10} g_N\ [\mathrm{ms}^{-2}]$
$\log_{10} g\ [\mathrm{ms}^{-2}]$

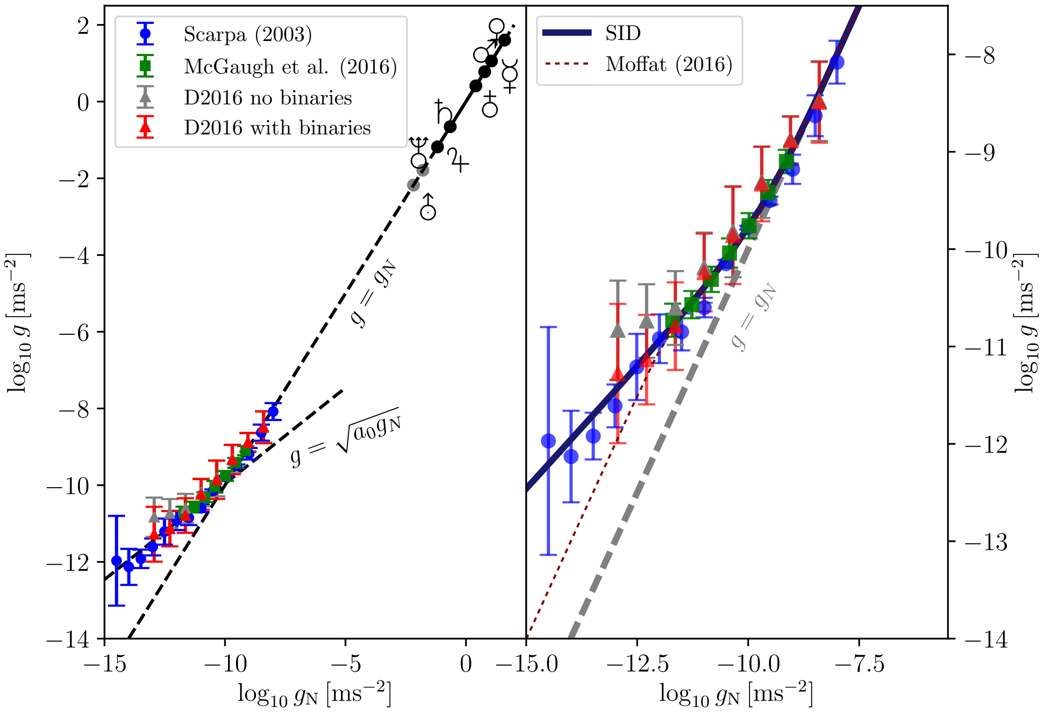

Mass-Discrepancy correlation with acceleration

McGaugh, Lelli & Schombert 2016, PRL

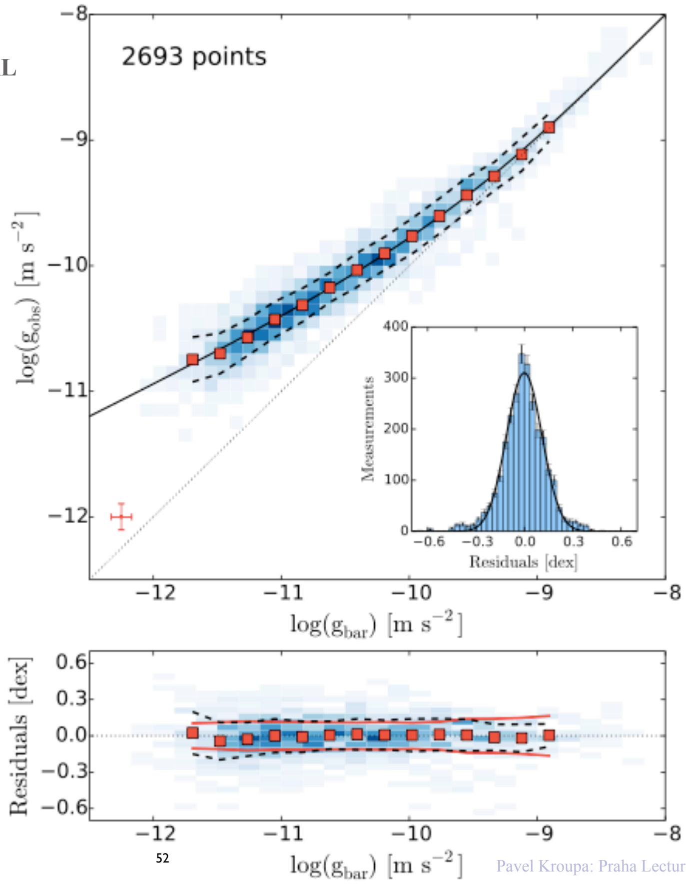

FIG. 3. The centripetal acceleration observed in rotation curves, $g_{obs} = V^2/R$, is plotted against that predicted for the observed distribution of baryons, $g_{bar} = |\partial\Phi_{bar}/\partial R|$ in the upper panel. Nearly 2700 individual data points for 153 SPARC galaxies are shown in grayscale. The mean uncertainty on individual points is illustrated in the lower left corner. Large squares show the mean of binned data. Dashed lines show the width of the ridge as measured by the rms in each bin. The dotted line is the line of unity. The solid line is the fit of eq. 4 to the unbinned data using an orthogonal-distance-regression algorithm that considers errors on both variables. The inset shows the histogram of all residuals and a Gaussian of width $\sigma = 0.11$ dex. The residuals are shown as a function of g_{obs} in the lower panel. The error bars on the binned data are smaller than the size of the points. The solid lines show the scatter expected from observational uncertainties and galaxy to galaxy variation in the stellar mass-to-light ratio. This extrinsic scatter closely follows the observed rms scatter (dashed lines): the data are consistent with negligible intrinsic scatter.

Mass-Discrepancy correlation with acceleration

Wu & Kroupa 2015

best (latest) CDM models

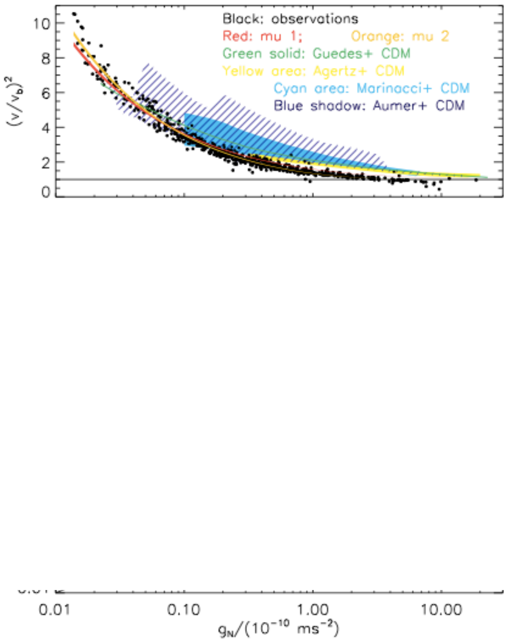

Mass-Discrepancy correlation with acceleration

Wu & Kroupa 2015

best (latest) CDM models

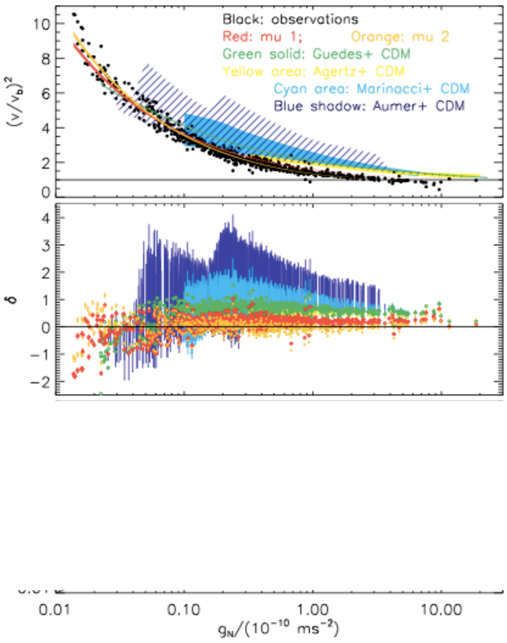

Mass-Discrepancy correlation with acceleration

Wu & Kroupa 2015

best (latest) CDM models

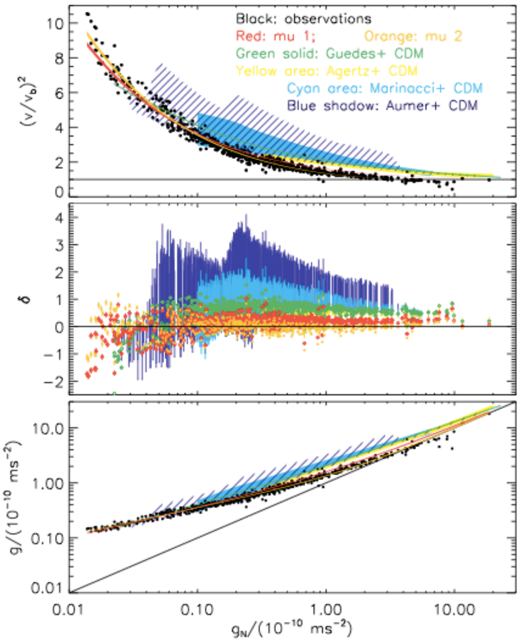

Mass-Discrepancy correlation with acceleration

Wu & Kroupa 2015

best (latest) CDM models

best (latest) WDM models

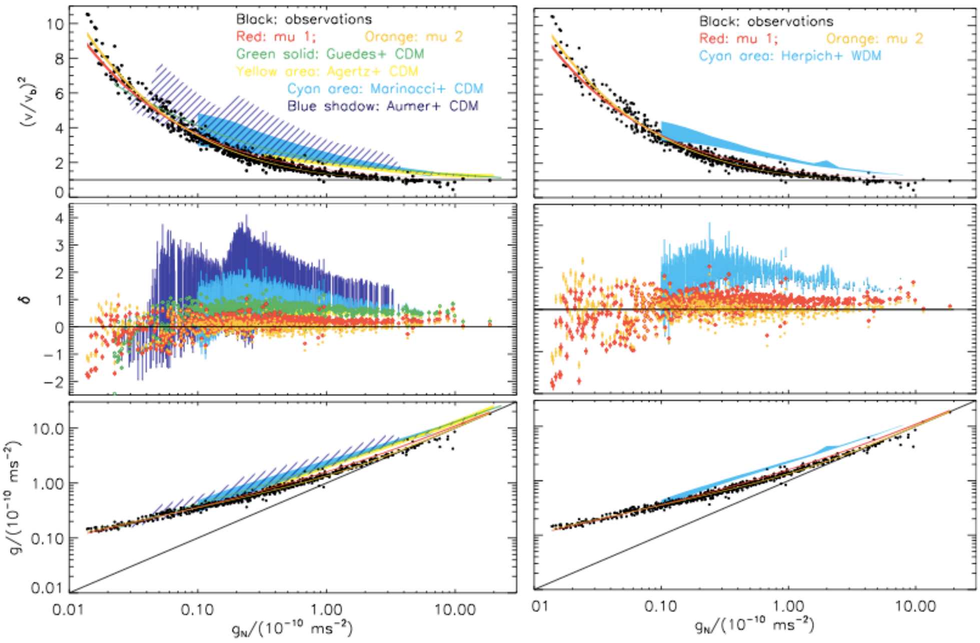

Mass-Discrepancy correlation with acceleration

Wu & Kroupa 2015

best (latest) CDM models   best (latest) WDM models

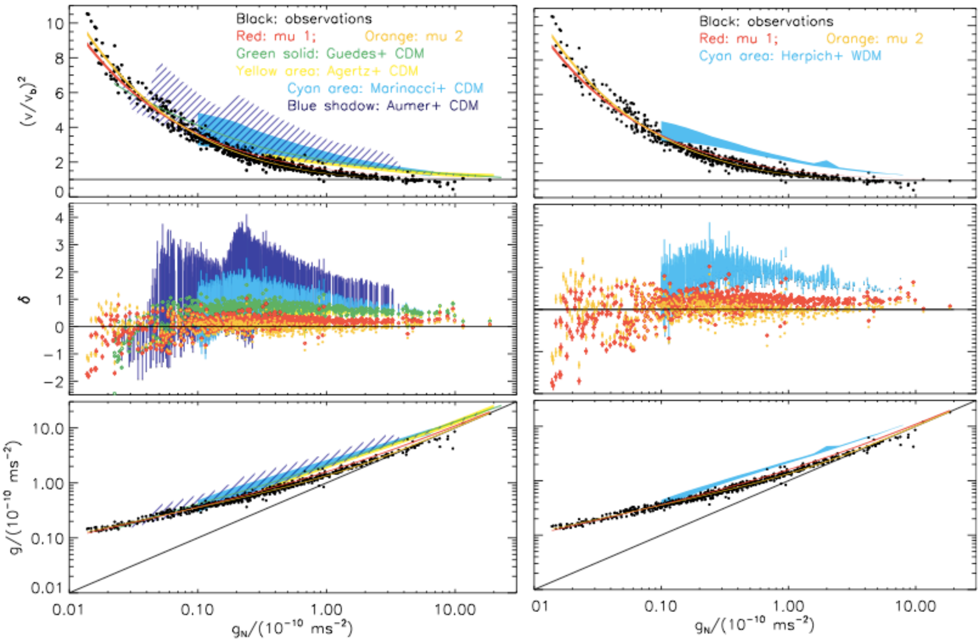

Correlation can't be explained by Dark Matter : DM particle physics is independent of the local acceleration in the SMoC.

Which law may account for the observed gravitational-dynamical behaviour ?

Consider *space-time scale invariance* :

(**Milgrom 2009**; Kroupa, Pawlowski & Milgrom 2012; Kroupa 2015)

If $(t, x, y, z) \longrightarrow \lambda(t, x, y, z)$

then, the Newtonian gravitational acceleration, $g_N \propto GM/r^2$,
scales as $g_N \longrightarrow \lambda^{-2} g_N$

while the kinematical acceleration, g , scales as $g \longrightarrow \lambda^{-1} g$ $\left[\frac{d\dot{x}}{dt}\right]$

For gravitational and kinematical acceleration to also be scale invariant we thus need g to scale as $g_N^{1/2}$

$$g = (a_o\, g_N)^{\frac{1}{2}}$$

$g^2 = a_o g_N$ or $a^2 = a_o g_N$

i.e. $\frac{a}{a_o} a = g_N$

space-time scale invariance (from above) :

i.e. $\frac{a}{a_o} a = g_N$, thus $a = \frac{\sqrt{GM}}{r}\sqrt{a_0}$

centrifugal acceleration = centripetal acceleration

$$a = \frac{V^2}{r} = \frac{\sqrt{GMa_0}}{r} \qquad (V \equiv V_c)$$

$$V = (GMa_0)^{\frac{1}{4}}$$

the ***Baryonic Tully-Fisher relation !***
and ***flat rotation curves !***

The observational Baryonic Tully -Fisher Relation

Famaey & McGaugh 2012

$V_f = (G\, a_0\, M_{bar})^{\frac{1}{4}}$

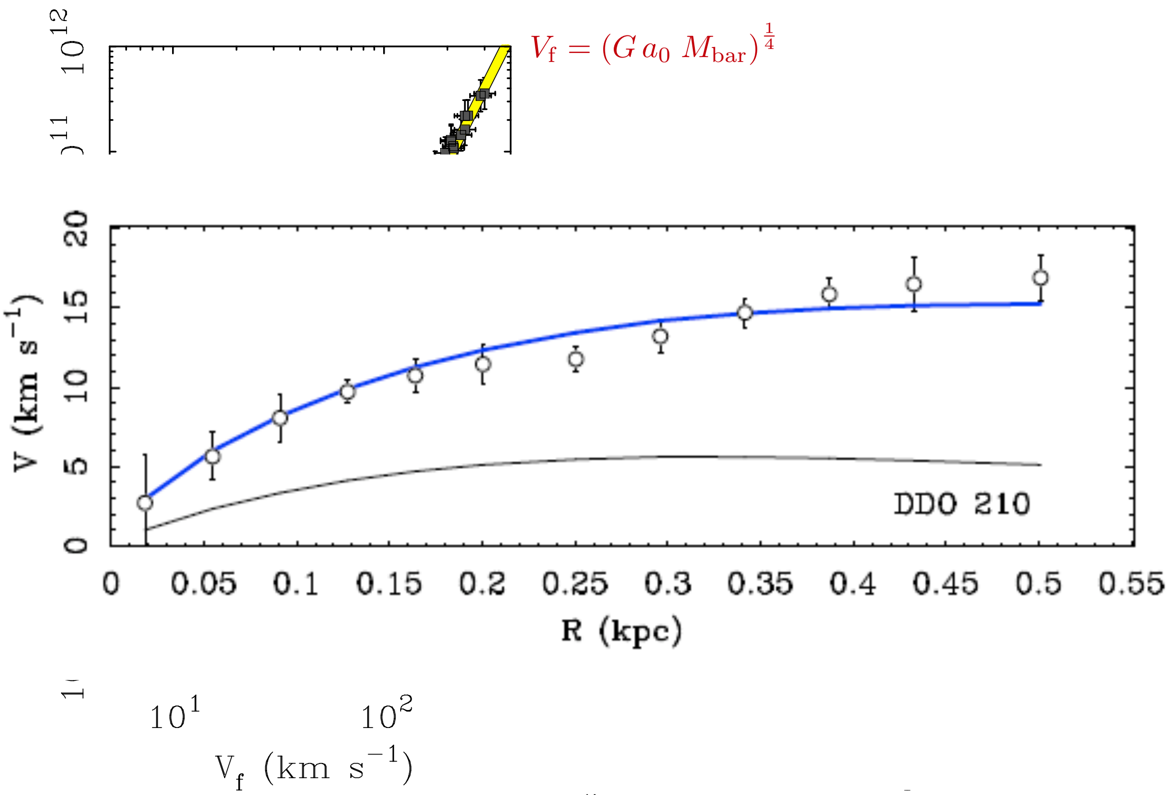

Consider *space-time scale invariance* :

(Milgrom 2009; Kroupa, Pawlowski & Milgrom 2012)

If $(t, x, y, z) \rightarrow \lambda(t, x, y, z)$

$g^2 = a_o g_N$

$g = (a_o\, g_N)^{\frac{1}{2}}$

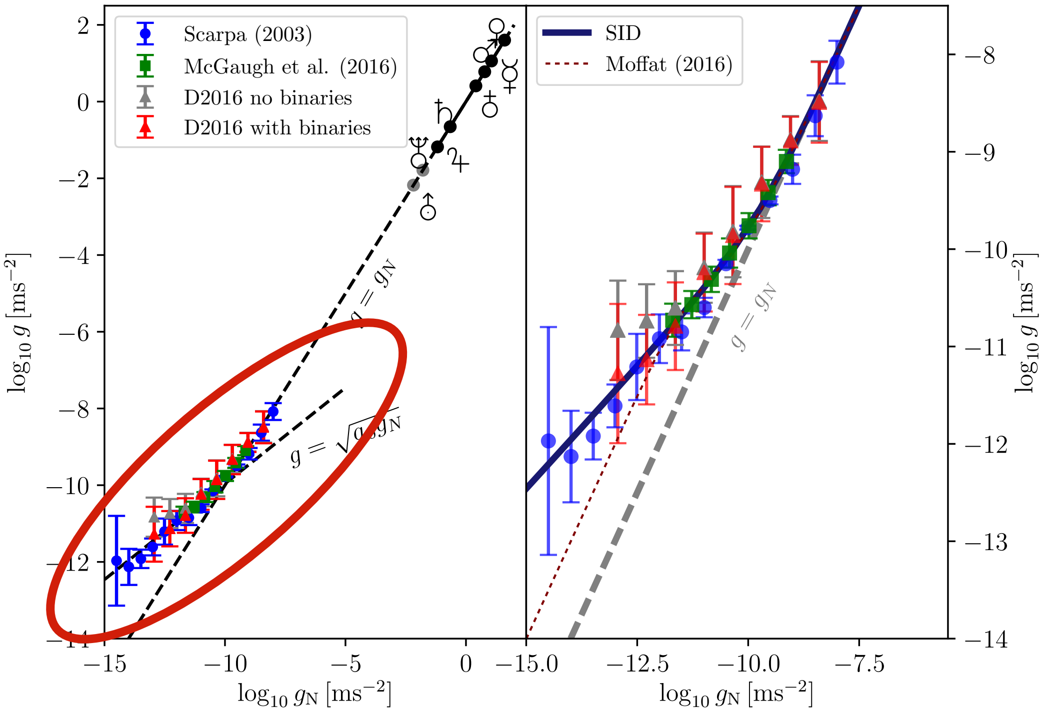

Consider *space-time scale invariance* :

(Milgrom 2009; Kroupa, Pawlowski & Milgrom 2012)

If $(t, x, y, z) \rightarrow \lambda(t, x, y, z)$

$\Rightarrow$ $g^2 = a_o g_N$ or $a^2 = a_o g_N$

i.e. $\frac{a}{a_o} a = g_N$

Since $V^2 = (G a_0 M)^{\frac{1}{2}}$

$$V_b^2 = \frac{GM}{r}$$

$\Rightarrow$
$$\left(\frac{V}{V_b}\right)^2 = \frac{(G a_0 M)^{\frac{1}{2}}}{r \frac{GM}{r^2}} = \frac{(G a_0 M)^{\frac{1}{2}}}{r a} = \left(\frac{a_0}{a}\right)^{\frac{1}{2}}$$

i.e. $\left(\frac{V}{V_b}\right)^2 = \left(\frac{a_0}{a}\right)^{\frac{1}{2}}$

Mass-Discrepancy correlation with acceleration

The Sanders-McGaugh correlation explained

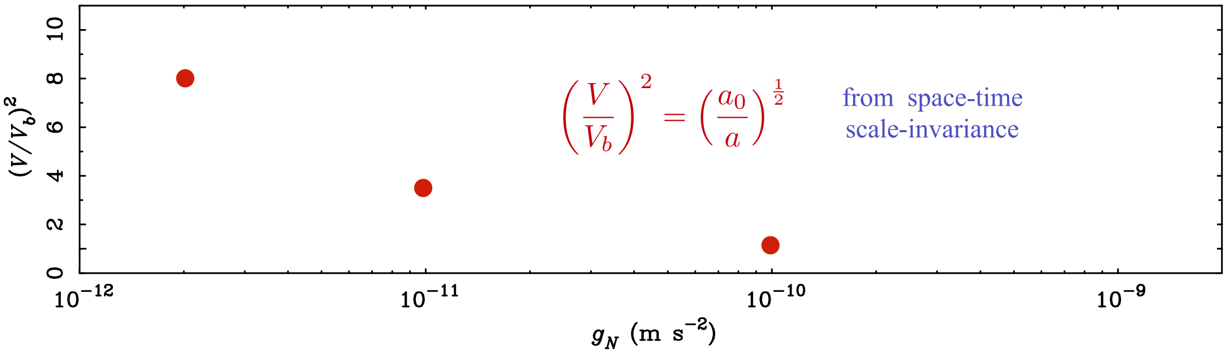

Mass-Discrepancy correlation with acceleration

The Sanders-McGaugh correlation explained

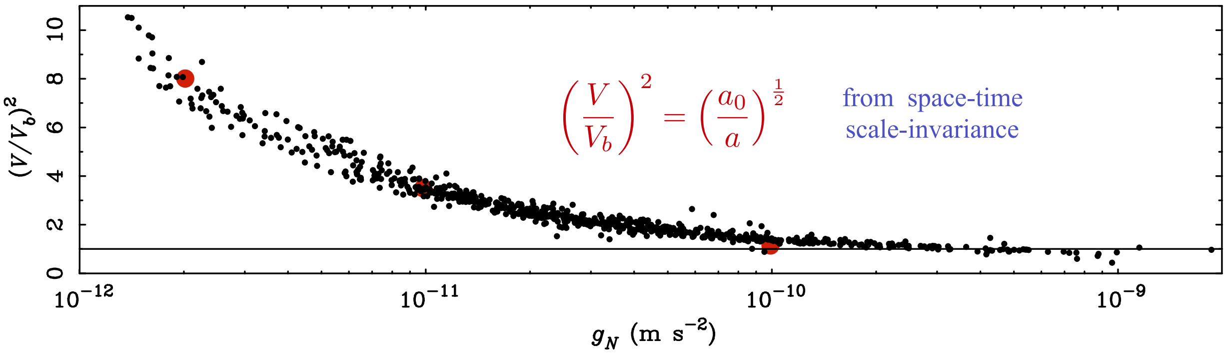

Mass-Discrepancy correlation with acceleration

The Sanders-McGaugh correlation explained

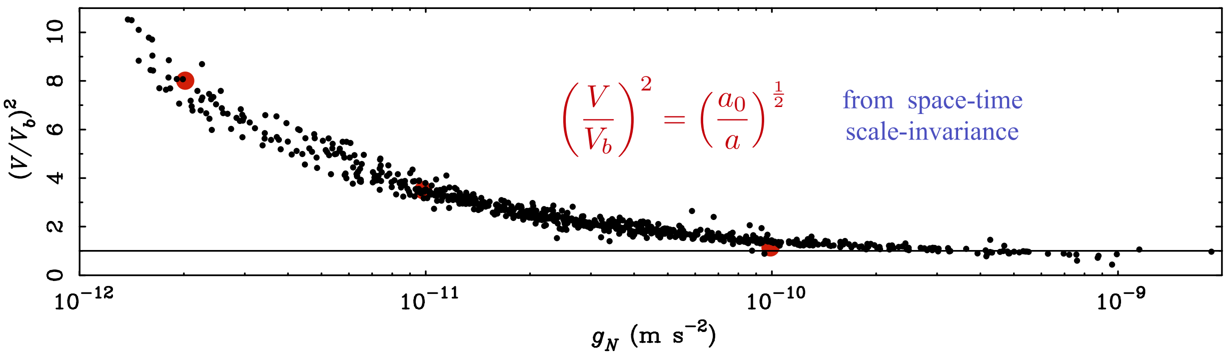

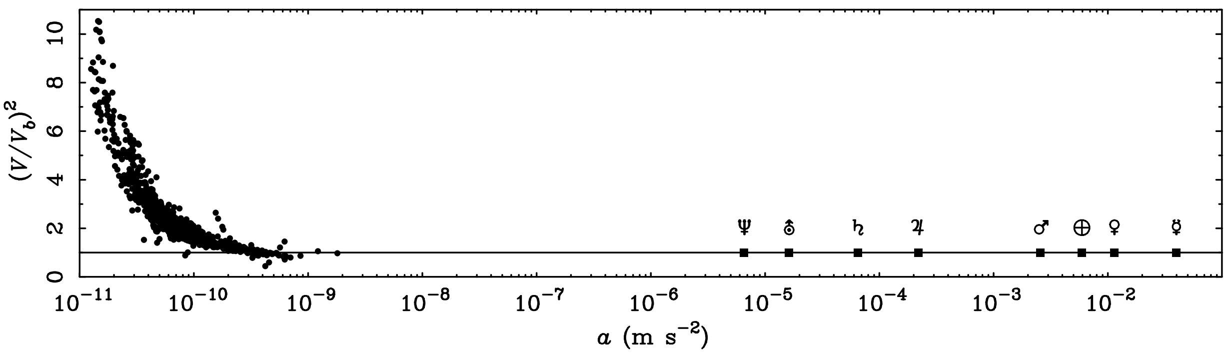

Galaxies follow the same law,
independently how they formed.

Exactly like planetary systems :
all follow the Kepler's laws,
independently how they formed.

Scale-Invariant or Milgromian dynamics in our current state of knowledge represents an effective empirical theory which is able to describe galaxies based on their baryonic content only.

It is already remarkable that something like this exists !

This may be viewed as an analogy to Kepler's or Newton's laws.

This we cannot argue against.

It is therefore worthwhile to seek a possible deeper theoretical understanding of Milgromian dynamics.

The data thus very strongly point towards a new law of nature (*scale-invariant dynamics* or *Milgromian dynamics*) in the regime of very weak space-time curvature.

Interesting possible connection with matter-free GR:

Conference *Cosmology on Small Scales 2016*
Michal Křížek and Yurii Dumin (Eds.)
Institute of Mathematics CAS, Prague

**SCALE INVARIANT COSMOLOGY:
COSMOLOGICAL MODELS AND SMALL SCALE EFFECTS**

2016arXiv160506315M

2016arXiv160506314M

2016arXiv160506314M

André Maeder

Geneva Observatory
chemin des Mailletes, CH-1290 Sauverny, Switzerland
andre.maeder@unige.ch

Abstract: We make the hypothesis that the empty space, at macroscopic and large scales, is scale invariant. This leads to essential simplifications in the cosmological equations with scale invariance. There is an additional term remaining that opposes to gravity and favors accelerated expansion. This term makes a significant contribution, called Ω_λ, to the energy-density of the Universe, satisfying an equation $\Omega_m + \Omega_k + \Omega_\lambda = 1$. Numerical integrations of

A lesson from history

How was the Planck black body radiation spectrum derived ?

"At the end of the Nineteenth Century any physicist who sought a theoretical understanding of blackbody radiation imagined heating a hollow body that had a small hole drilled in its side. That physicist then imagined that the cavity inside that body contained a large number of electromagnetic dipole resonators of undetermined composition: absorbing and re-emitting radiation more or less at random, those resonators mixed the radiation to ensure that it filled all of the modes of electromagnetic vibration available inside the cavity.

Classical electromagnetic theory, completed by James Clerk Maxwell (1831 Jun 13 - 1879 Nov 05) in the 1860's, provides a straightforward means of calculating the number of vibrational modes inside the cavity."

But the theory implied a ultraviolet catastrophe (infinite energy density at short wavelengths), which was not measured.

Essentially, Planck found an interpolation formula between Wien's spectral energy distribution law (at high frequencies) and the Rayleigh-Jeans law (at low frequencies).

By doing so he had to introduce an auxiliary parameter, h, ("Hilfsgroesse" in German).

At that time, in 1900, no-one knew that this was essentially a constant of energy quantisation.

"Thus Planck laid the cornerstone upon which he and other physicists of the early Twentieth Century built the grand edifice of the Quantum Theory."

(from http://bado-shanai.net/Map%20of%20Physics/mopPlancksderivBRL.htm)

Today

How was Milgromian gravitational dynamics derived ?

At the end of the Twentieth Century any physicist who sought a theoretical understanding of gravitation, imagined it to be a geometrical distortion of space time aided by unseen dark matter particles.

The general theory of relativity, published by Albert Einstein in 1916, provides a "straightforward" means of calculating gravitational effects around any mass concentration.

But the theory implied galactic dynamics processes (e.g. dynamical friction) not observed and wrong galactic rotation curves.

Essentially, Milgrom found an interpolation formula between Newton's "universal" law of gravitation (nearby gravitating bodies) and the effective (Newtonian) isothermal-potential law (at very low accelerations).

"Thus Milgrom laid the cornerstone upon which he and other physicists of the early Twentyfirst Century built the grand edifice of the **....?....** Theory."

(e.g. Famaey & McGaugh 2010; Kroupa 2015)

The data thus very strongly point towards a new law of nature (*scale-invariant dynamics* or *Milgromian dynamics*) in the regime of very weak space-time curvature.

ELSEVIER

29 March 1999

PHYSICS LETTERS A

Physics Letters A 253 (1999) 273–279

This property of Minkowski space may be due to quantum-mechanical processes in the vacuum :

The modified dynamics as a vacuum effect

Mordehai Milgrom

Department of Condensed Matter Physics, Weizmann Institute, Rehovot, Israel

Received 17 August 1998; revised manuscript received 4 January 1999; accepted for publication 25 January 1999
Communicated by P.R. Holland

Abstract

To explain the appearance in MOND of a cosmological acceleration constant, a_0, I suggest that MOND inertia – as embodied in the actions of free particles and fields – is due to effects of the vacuum. The same vacuum effects enter both MOND (through a_0) and cosmology (e.g. through a cosmological constant Λ). For example, a constant-acceleration (a) observer in de Sitter universe sees Unruh radiation of temperature $T \propto [a^2 + a_0^2]^{1/2}$, with $a_0 \equiv (\frac{1}{3}\Lambda)^{1/2}$, and I note that $T(a) - T(0)$ depends on a in the same way that MOND inertia does. © 1999 Published by Elsevier Science B.V.

Milgromian Dynamics
from quantum mechanical processes in the vacuum

Kroupa et al. (2010), Appendix A (see Milgrom 1999) :

"... an accelerated observer in a de Sitter universe (curved with a positive cosmological constant Λ) sees a non-linear combination of the Unruh (1975) vacuum radiation and of the Gibbons & Hawking (1977) radiation due to the cosmological horizon in the presence of a positive Λ. Milgrom (1999) then defines inertia as a force driving such an observer back to equilibrium as regards the vacuum radiation (i.e. experiencing only the Gibbons-Hawking radiation seen by a non-accelerated observer).
Observers experiencing *a very small acceleration* would thus see an Unruh radiation with a low temperature close to the Gibbons-Hawking one, meaning that *the inertial resistance defined by the difference between the two radiation temperatures would be smaller than in Newtonian dynamics, and thus the corresponding acceleration would be larger*. This is given precisely by the formula of Milgrom (1983) with a well-defined transition-function $\mu(x)$, and $a_0 = c\,(\Lambda/3)^{1/2}$. Unfortunately, no covariant version (if at all possible) of this approach has been developed yet."

Milgromian Dynamics

Ansatz : (Milgrom 1983, ApJ, 270, 371)

$$\mu\left(\frac{a}{a_0}\right)\vec{a} = \vec{g_\mathrm{N}} \quad \begin{cases} \mu(x) = 1 \text{ if } |x| \gg 1 \\ \mu(x) = x \text{ if } |x| \ll 1 \end{cases}$$

i.e. $\vec{a} = \vec{g_\mathrm{N}}\,\mu^{-1} \geq \vec{g_\mathrm{N}}$

What is the transition function $\mu(x)$ **?**

$$\mu(x) = \frac{x}{(1+x^2)^{\frac{1}{2}}} \qquad x = \frac{a}{a_0}$$

Empirical constraints from combination of Solar system and Galactic observations :

Hees, Famaey et al. 2016, MNRAS)

Effects on the outer Solar System :

"Sedna and the cloud of comets ..."

Pauco & Klacka (Bratislawa) 2016,A&A)

(Milgrom 1999, Physics Letters A)

Note here that the quantity $a(\partial T/\partial a)$, which measures e.g. the temperature change under small dilatations of the orbit, also gives a MOND-like expression

$$a\frac{\partial T}{\partial a} = a\mu(a/a_0), \qquad (10)$$

$$\mu(x) = x/(1+x^2)^{1/2}, \qquad (11)$$

and $a_0 = (\frac{1}{3}\Lambda)^{1/2}$, although the significance of this is, again, not clear.

Milgromian Dynamics

Ansatz : (Milgrom 1983, ApJ, 270, 371)

$$\mu\left(\frac{a}{a_0}\right)\vec{a} = \vec{g_\mathrm{N}} \quad \begin{cases} \mu(x) = 1 \text{ if } |x| \gg 1 \\ \mu(x) = x \text{ if } |x| \ll 1 \end{cases}$$

i.e. $\vec{a} = \vec{g_\mathrm{N}}\,\mu^{-1} \geq \vec{g_\mathrm{N}}$

Thus,

$$\vec{g_\mathrm{N}} = \mu\left(\frac{a}{a_0}\right)\vec{a} \;\rightarrow\; \frac{GM}{r^2} = \mu\left(\frac{a}{a_0}\right)a$$

For $a < a_0$: $\mu\left(\frac{a}{a_0}\right) = \frac{a}{a_0} \;\rightarrow\; \frac{GM}{r^2} = \frac{a^2}{a_0}$ and $a = \frac{\sqrt{GMa_0}}{r}$

centripetal = centrifugal acceleration $a = \frac{v^2}{r} = \frac{\sqrt{GMa_0}}{r}$ $(v \equiv v_c)$

♣ $\boxed{v = (GMa_0)^{\frac{1}{4}}}$ the ***Baryonic Tully-Fisher relation***

Milgromian Dynamics

Ansatz : (Milgrom 1983, ApJ, 270, 371)

$$\mu\left(\frac{a}{a_0}\right)\vec{a}=\vec{g_{\rm N}} \quad \left\{ \begin{array}{l} \mu(x)=1 \text{ if } |x|\gg 1 \\ \mu(x)=x \text{ if } |x|\ll 1 \end{array}\right.$$

i.e. $\vec{a}=\vec{g_{\rm N}}\,\mu^{-1}\geq\vec{g_{\rm N}}$

What is the interpretation ?

Milgromian dynamics can be understood to be

a different effective Law of Gravity

through a generalised "Poisson" equation

$$\vec{\nabla}\cdot\left[\mu\left(\frac{|\vec{\nabla}\phi|}{a_0}\right)\vec{\nabla}\phi\right]=4\pi\,G\,\rho$$

giving the Milgromian potential

a modification of the Law of Inertia

through the breaking of the equivalence of inertial and gravitating mass

$$\vec{a}=\vec{F}\left[m\,\mu\left(\frac{|\vec{\nabla}\phi|}{a_0}\right)\right]^{-1}$$

where $\vec{F}=m\,\vec{g_{\rm N}}$ for gravity

The data thus very strongly point towards a new law of nature (*scale-invariant dynamics* or *Milgromian dynamics*) in the regime of very weak space-time curvature.

A formulation in the classical limit is known and is energy and momentum conserving **:**

Bekenstein & Milgrom (1984, ApJ)

The field equation (3) is analogous to the equation for the electrostatic potential in a nonlinear isotropic medium in which the dielectric coefficient is a function of the electric field strength.

It may also be useful to note that our field equation is equivalent to the stationary flow equations of an irrotational fluid which has a density $\hat{\rho}=\mu(|\nabla\varphi|/a_0)$, a negative pressure $\hat{P}=-2^{-1}a_0^2\mathscr{F}[(\nabla\varphi)^2/a_0^2]$, flow velocity $\hat{\boldsymbol{v}}=\nabla\varphi$, and a source distribution $\hat{S}(r)=4\pi G\rho$. The fluid satisfies an equation of state $\hat{P}(\hat{\rho})=-2^{-1}a_0^2\mathscr{F}\{[\mu^{-1}(\hat{\rho})]^2\}\equiv f(\hat{\rho})$.

An equation of the same form as equation (3) has been studied in a different context to describe classical models of quark confinement using a very different form of the function μ at both large and small values of its argument (see Adler and Piran 1984 and also Lehman and Wu 1983 for a review).

II. THE FIELD EQUATIONS

In Newtonian gravity test bodies move with an acceleration equal to $\boldsymbol{g}_{\rm N}=-\nabla\varphi_{\rm N}$, where $\varphi_{\rm N}$ is the Newtonian gravitational potential. It is determined by the Poisson equation $\nabla^2\varphi_{\rm N}=4\pi G\rho$, where ρ is the mass density which produces $\varphi_{\rm N}$. The Poisson equation may be derived from the Lagrangian

$$L_{\rm N}=-\int d^3r\{\rho\varphi_{\rm N}+(8\pi G)^{-1}(\nabla\varphi_{\rm N})^2\}\,. \qquad (2a)$$

In searching for a modification of this theory we will want to retain the notion of a *single* potential φ from which acceleration derives. And, as in Newtonian gravity, it is desirable that φ be arbitrary up to an additive constant. The most general modification of $L_{\rm N}$ which will yield these features is

$$L=-\int d^3r\left\{\rho\varphi+(8\pi G)^{-1}a_0^2\mathscr{F}\left[\frac{(\nabla\varphi)^2}{a_0^2}\right]\right\}, \qquad (2b)$$

where $\mathscr{F}(x^2)$ is an arbitrary function. Note that a scale of acceleration is necessary unless we are in the Newtonian case.

Variation of L with respect to φ with variation of φ vanishing on the boundary yields

$$\nabla\cdot[\mu(|\nabla\varphi|/a_0)\nabla\varphi]=4\pi G\rho\,, \qquad (3)$$

with $\mu(x)=\mathscr{F}'(x^2)$, as the equation determining the modified potential. A test particle is assumed to have acceleration $\boldsymbol{g}=-\nabla\varphi$. We supplement equation (3) by the boundary condition $|\nabla\varphi|\to 0$ as $r\to\infty$.

In fact, given an *observed baryonic matter distribution*, the rotation curve

can be precisely predicted using Milgromian dynamics

cannot be predicted using LCDM.

plus in Milgromian dynamics dark matter significantly reduced in galaxy clusters

→ (e.g. Sanders 2009 (review) : "*Modified Newtonian Dynamics : A Falsification of Cold Dark Matter*")

How successful is Milgromian gravitation compared to observations ?

Perform simulations of galaxy formation with gas dynamics, star formation and feedback, i.e. full-scale baryonic processes, using the computer code Phantom of Ramses (PoR, Lueghausen, Famaey & Kroupa 2014, CJP).

MNRAS **463,** 3637–3652 (2016)
Advance Access publication 2016 September 14
doi:10.1093/mnras/stw2331

Star formation triggered by galaxy interactions in modified gravity

Florent Renaud,[1★] Benoit Famaey[2] and Pavel Kroupa[3,4]

[1] *Department of Physics, University of Surrey, Guildford GU2 7XH, UK*
[2] *Observatoire Astronomique de Strasbourg, Université de Strasbourg, CNRS UMR 7550, 11 rue de l'Université, F-67000 Strasbourg, France*
[3] *Helmholtz-Institut für Strahlen- und Kernphysik, Nussallee 14-16, D-53115 Bonn, Germany*
[4] *Astronomical Institute, Faculty of Mathematics and Physics, Charles University in Prague, V Holešovičkách 2, CZ-180 00 Praha 8, Czech Republic*

Accepted 2016 September 12. Received 2016 September 12; in original form 2016 July 24

ABSTRACT

Together with interstellar turbulence, gravitation is one key player in star formation. It acts both at galactic scales in the assembly of gas into dense clouds and inside those structures for their collapse and the formation of pre-stellar cores. To understand to what extent the large-scale dynamics govern the star formation activity of galaxies, we present hydrodynamical simulations in which we generalize the behaviour of gravity to make it differ from Newtonian dynamics in the low-acceleration regime. We focus on the extreme cases of interacting galaxies, and compare the evolution of galaxy pairs in the dark matter paradigm to that in the Milgromian dynamics (MOND) framework. Following up on the seminal work by Tiret & Combes, this paper documents the first simulations of galaxy encounters in MOND with a detailed Eulerian hydrodynamical treatment of baryonic physics, including star formation and stellar feedback. We show that similar morphologies of the interacting systems can be produced by both the dark matter and MOND formalisms, but require a much slower orbital velocity in the MOND case. Furthermore, we find that the star formation activity and history are significantly more extended in space and time in MOND interactions, in particular in the tidal debris. Such differences could be used as observational diagnostics and make interacting galaxies prime objects in the study of the nature of gravitation at galactic scales.

 (2016)

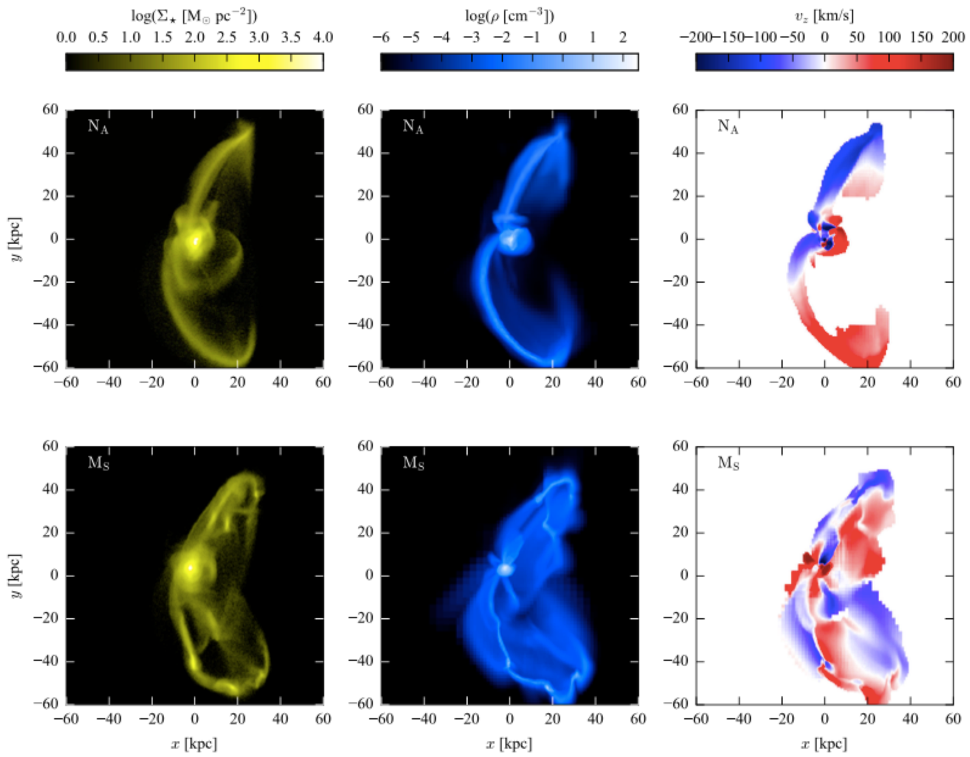

Figure 3. Map of the stellar surface density (left), gas density (centre) and velocity along the line of sight (right) of the N_A (top) and M_S (bottom), at the second pericentre passage. For the sake of clarity, only the velocity field in regions of high gas density is shown.

Note the sharper and more structured features due to the baryons self- gravity in the MOND (M_S), compared to the Newtonian (N_A) one.

--> relevant for Magellanic Stream !!

Galaxy formation and evolution: (Wittenburg, 2016/17, MSc thesis)

The evolution over 10 Gyr of a spherical gas cloud of mass $M_{gas} = 6.4 \times 10^9$ $M_\odot$ and $r_{sph} = 20$ kpc and with an initial cylindrical rotational law with $\eta = 0.025$ Myr^{-1} :

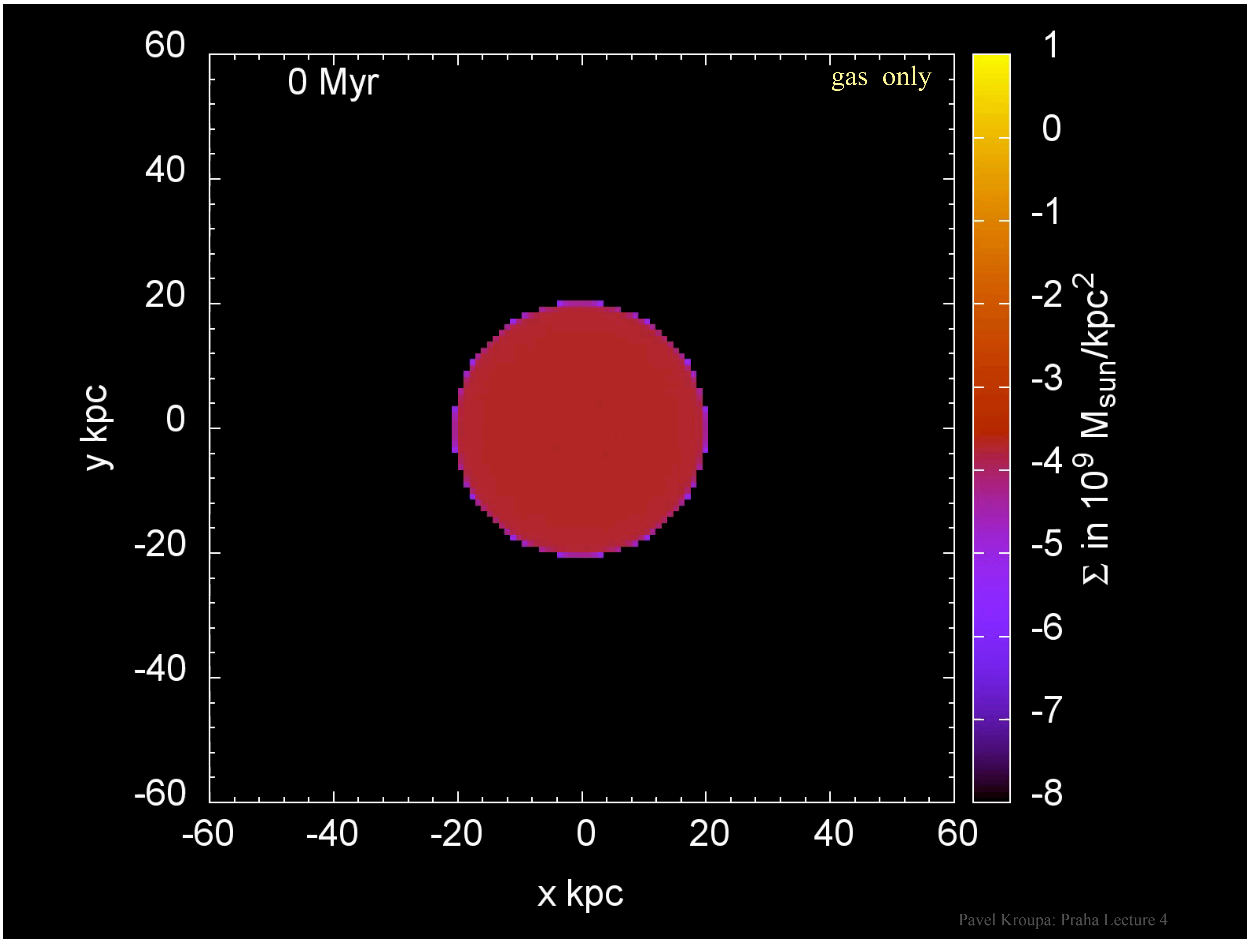

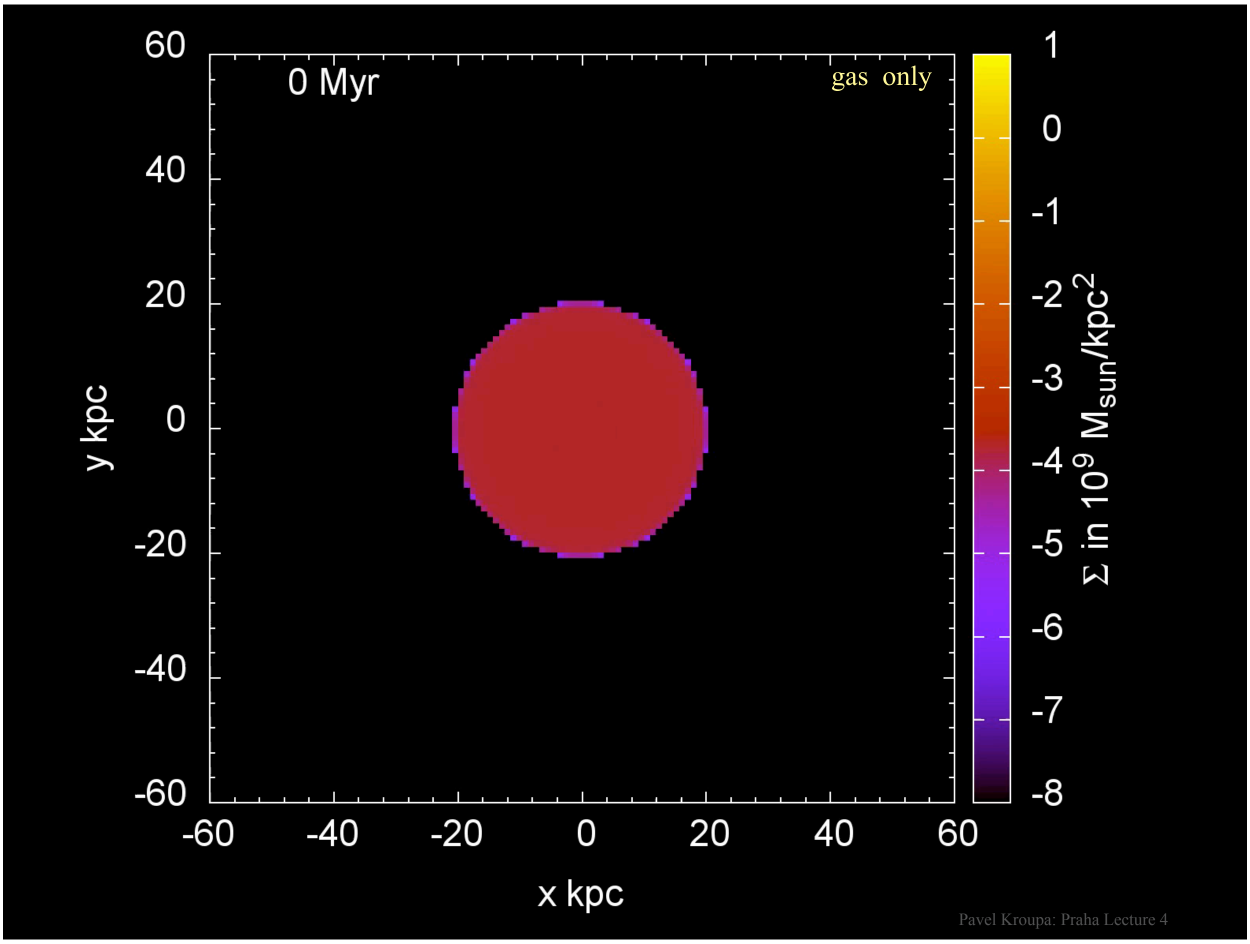
0 Myr
gas only
y kpc
x kpc
Σ in 10^9 Msun/kpc^2
Pavel Kroupa: Praha Lecture 4

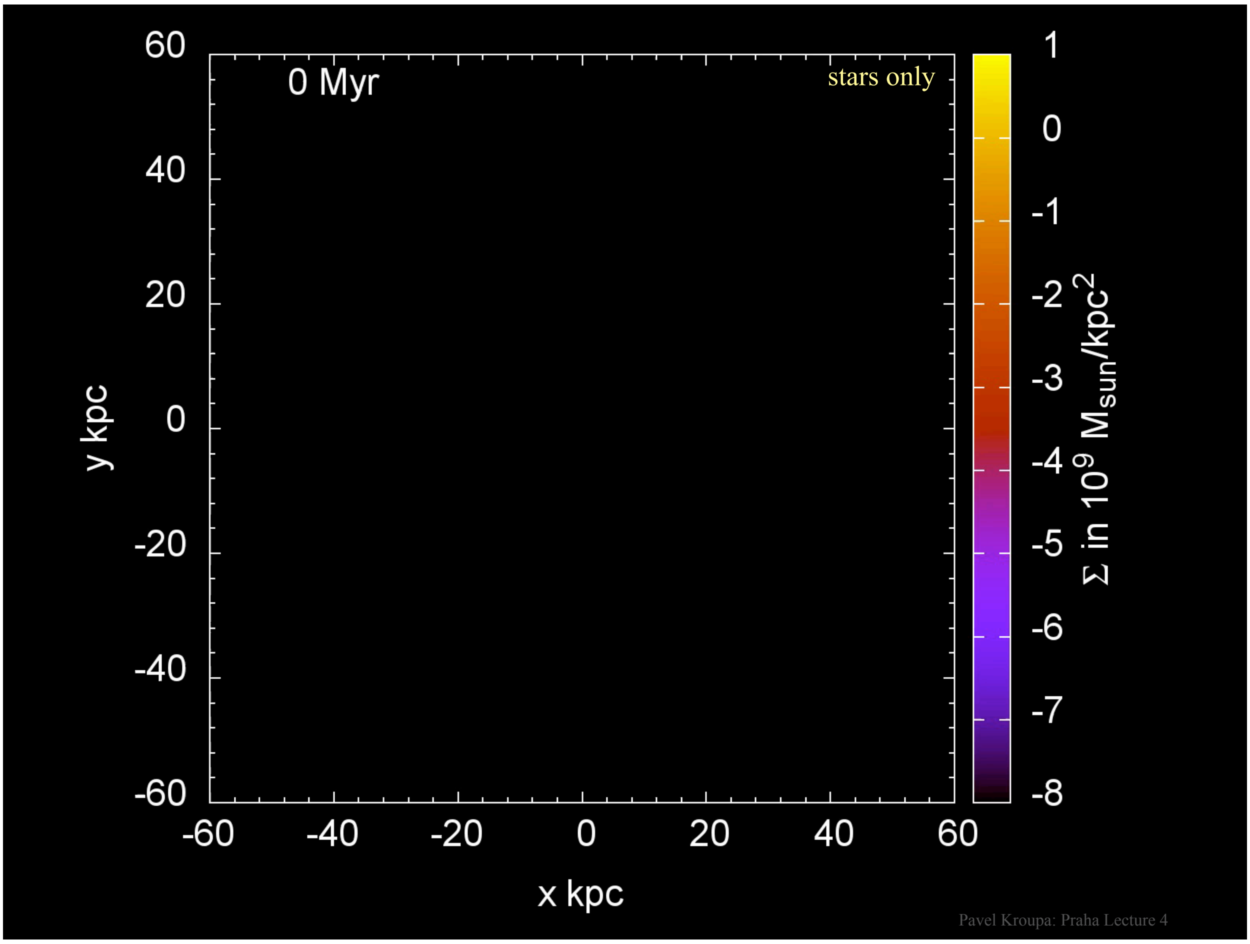
0 Myr
stars only
y kpc
x kpc
Σ in 10^9 Msun/kpc^2
Pavel Kroupa: Praha Lecture 4

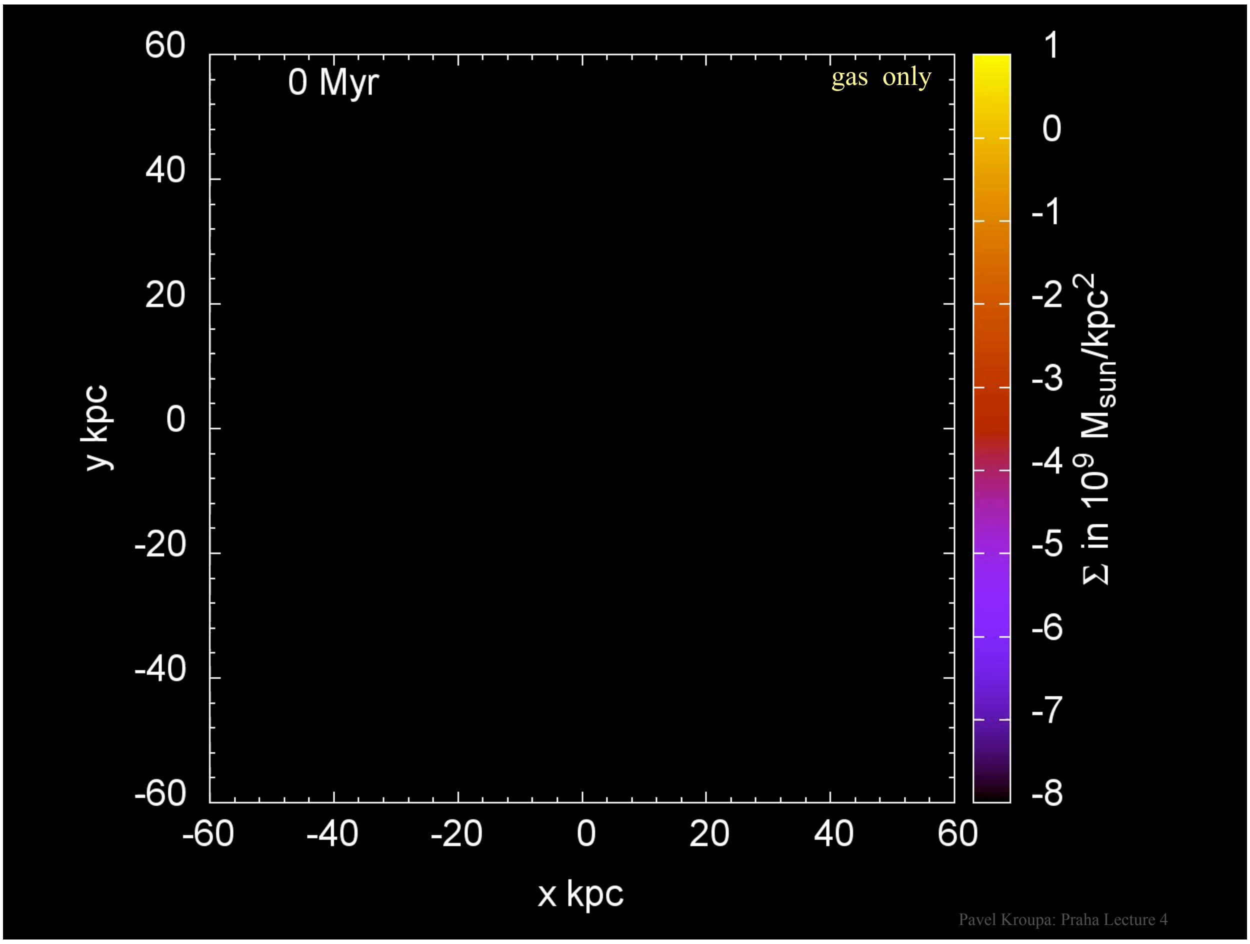

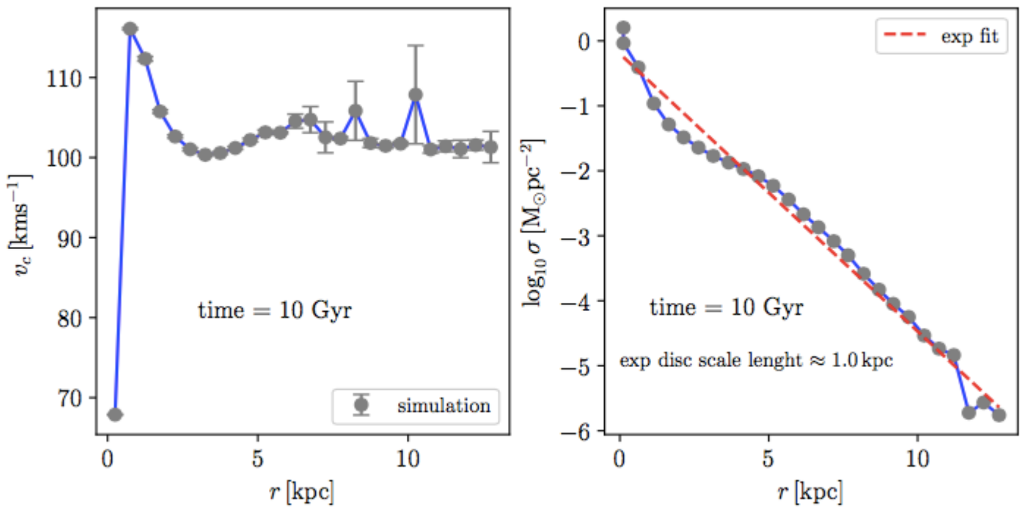

Model galaxies lie on BTFR, have flat rotation curves, follow Renzo's rule and have exponential surface density profiles.

Naturally !

Results are not very sensitive to the algorithms for baryonic processes !

Formation and evolution of a compact group of galaxies :

(Wittenburg, 2016/17, MSc thesis)

The model begins with an initially 10^4 K warm spherical gas cloud of mass $M_{gas} = 10^{11}\, M_\odot$, initial radius of $r_{sph} = 50$ kpc and with an initial cylindrical rotational law $v_{circ} = \eta\, R$, $\eta = 0.1\ \mathrm{Myr}^{-1}$.

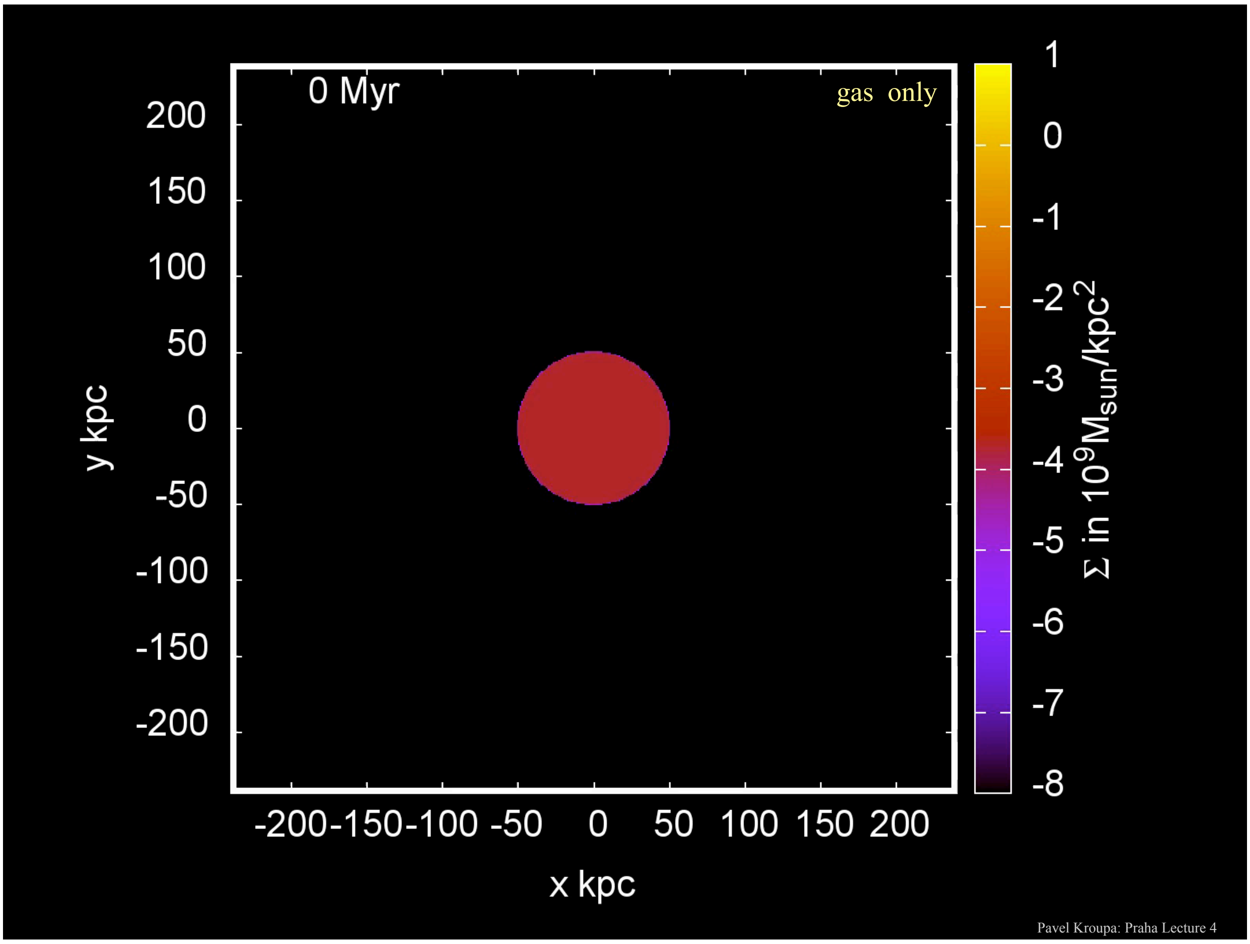

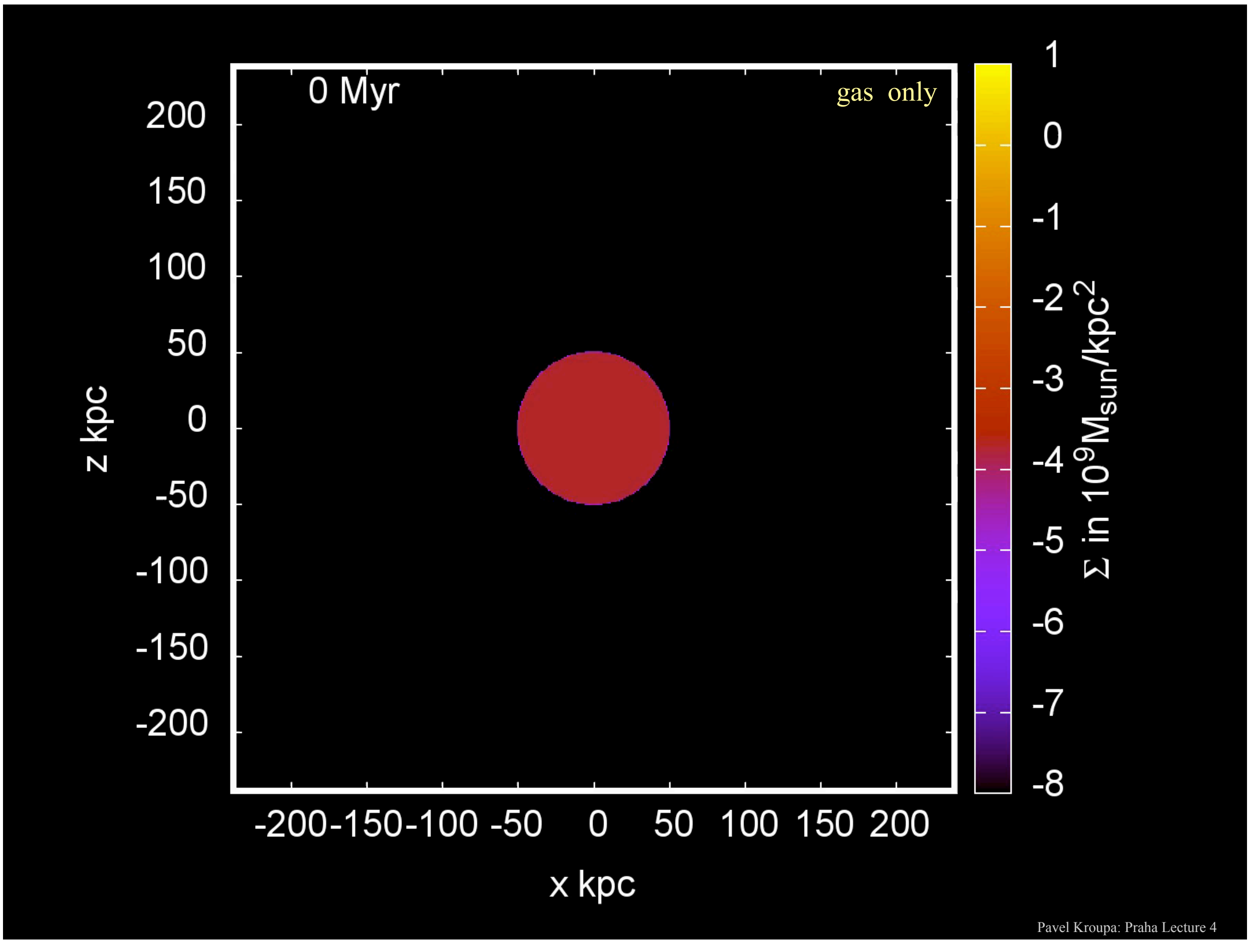
0 Myr
gas only
z kpc
200
150
100
50
0
-50
-100
-150
-200
-200 -150 -100 -50 0 50 100 150 200
x kpc
1
0
-1
-2
-3
-4
-5
-6
-7
-8
Σ in 10^9 M_sun/kpc^2
Pavel Kroupa: Praha Lecture 4

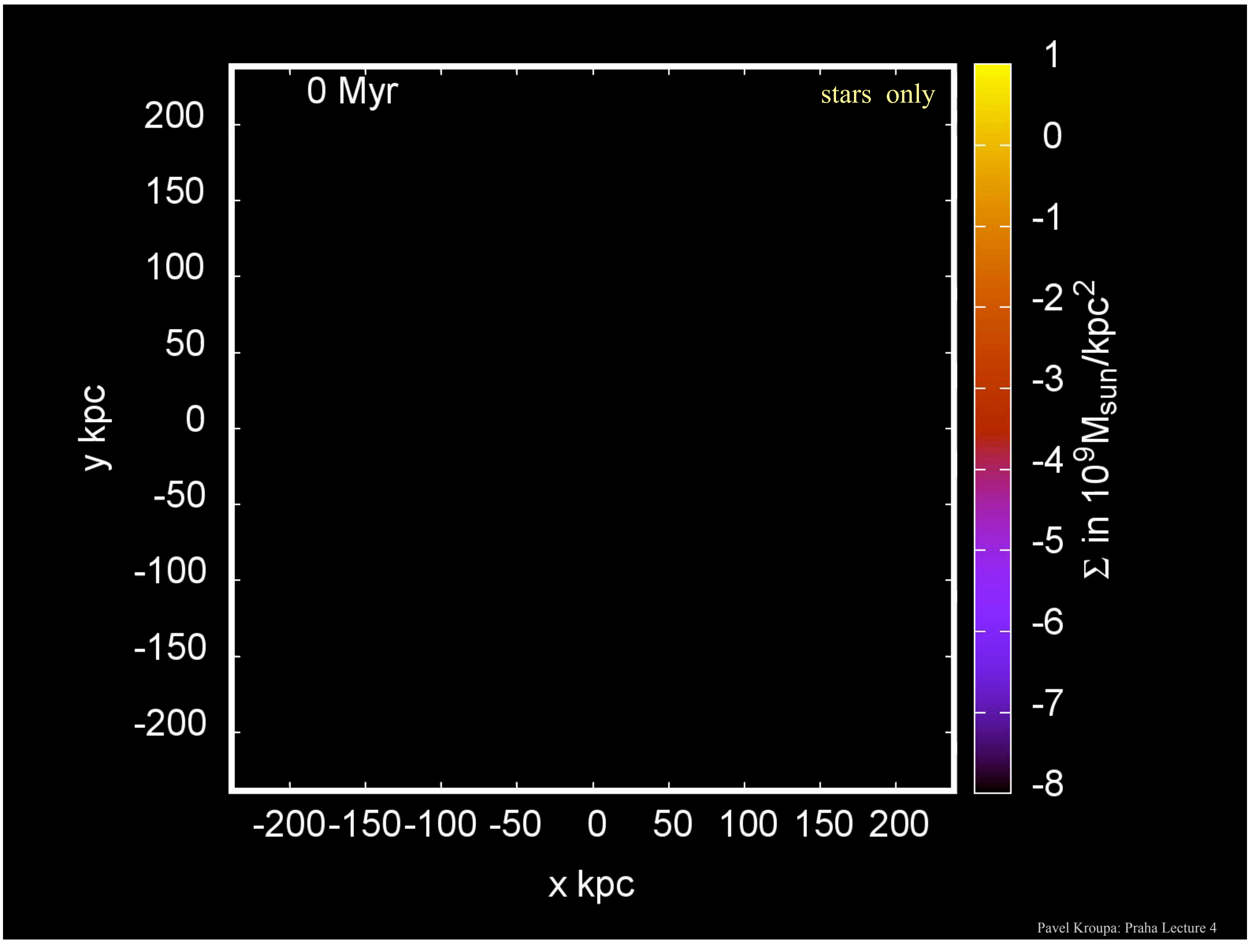
0 Myr
stars only
y kpc
200
150
100
50
0
-50
-100
-150
-200
-200 -150 -100 -50 0 50 100 150 200
x kpc
1
0
-1
-2
-3
-4
-5
-6
-7
-8
Σ in 10^9 M_sun/kpc^2
Pavel Kroupa: Praha Lecture 4

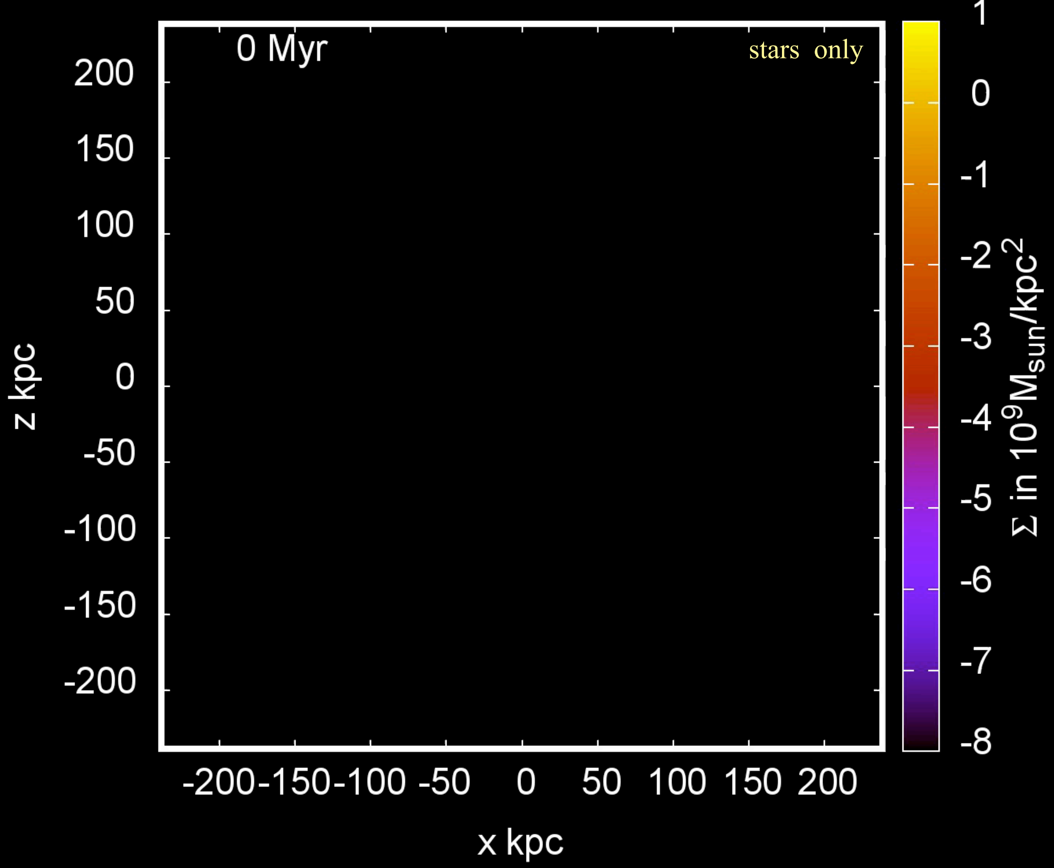

Hickson Compact Group 40

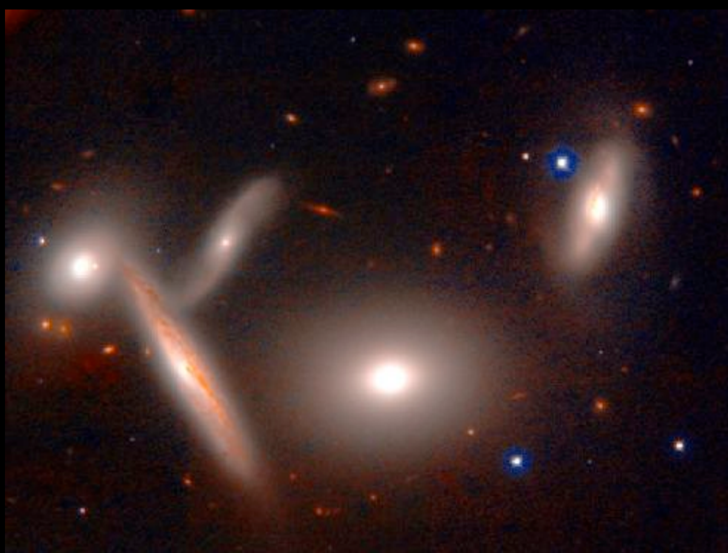

… in the real Universe and in Milgromian dynamics, galaxies merge rarely

Formation and evolution of galaxies in MOND :

(Wittenburg, 2016/17, MSc thesis)

These computations show :

1) Exp. disks arise naturally.
2) The model galaxies are on the BTFR.
3) Details of baryonic physics are not decisive.
4) Very early (<1Gyr) disk galaxies appear.
5) During the formation of a compact group of galaxies, the early merging (due to gas dissipation) evolves into a long-lived compact group without significant later merging (due to lack of dark matter halo).

Mordecai Milgrom
(+PK)
Strasbourg, 29.06.2010.

Ansatz :

(Milgrom 1983, ApJ, 270, 371)

END of Lecture 4